# Atmospheric fluxes of soluble organic C, N, and P to the Mediterranean Sea: Potential biogeochemical implications in the surface layer

K. Djaoudi, France van Wambeke, A. Barani, S. Hélias Nunige, Richard Sempere, E. Pulido-Villena

# Atmospheric fluxes of soluble organic C, N, and P to the Mediterranean Sea: potential biogeochemical implications in the surface layer

Djaoudi*, K., Van Wambeke, F., Barani, A., Hélias-Nunige, S., Sempéré, R., Pulido-Villena, E.

Aix-Marseille Université, Mediterranean Institute of Oceanography (MIO) UMR 7294, Université de Toulon, CNRS, IRD, France.

*Corresponding author. Tel: +33 4 86 09 05 36

*E-mail address: kahina.djaoudi@mio.osupytheas.fr

Progress in Oceanography, Elsevier, 2017, 10.1016/j.pocean.2017.07.008

## Abstract

Linking atmospheric deposition to marine carbon and nutrient cycle is hampered by the lack of data on atmospheric fluxes of organic matter. To fill this gap, this study reports the first quantification of atmospheric fluxes of soluble organic carbon (SOC), nitrogen (SON) and phosphate (SOP) to the NW Mediterranean Sea. Simultaneous measurements of dissolved organic carbon (DOC), dissolved organic nitrogen (DON) and dissolved organic phosphate (DOP) in the surface mixed layer (SML) allowed estimating the potential contribution of atmospheric fluxes to marine DOC, DON and DOP inventories. We found an annual atmospheric flux of 59 mmol C $m^{-2}$ $year^{-1}$ for SOC, 16.4 mmol N $m^{-2}$ $year^{-1}$ for SON and 23.6 µmol P $m^{-2}$ $year^{-1}$ for SOP, with proportions of SON and SOP to total soluble nitrogen and phosphate of 40% and 25%, respectively. Assuming these annual fluxes valid for the entire western Mediterranean basin, atmospheric fluxes would be higher than DOC, DON and DOP fluxes from the Rhône River by a factor of 6, 17 and 2, for C, N and P, respectively, which highlights the importance of atmospheric deposition as a source of DOC, DON and DOP to surface waters of the western Mediterranean Sea. Inventories of DOC, DON and DOP in the surface mixed layer displayed similar trends over the study period with maximum values at the end of the stratification period. DOP inventories contributed by 85 ± 11% to total dissolved phosphate (TDP) pool and exhibited a labile fraction (LDOP) of 27 ± 19%. The contribution of atmospheric SOC, SON and SOP to the DOC, DON and DOP pools in the SML were estimated for the stratification period, and suggested a low contribution of SOC to DOC pool (3%) and moderate contributions of both SON and SOP to DON (12%) and DOP (4.5%) pools for this period of time, respectively. The labile fraction of SOP (LSOP) was quantified throughout the sampling period and showed a high variability ranging from 0 to 97%. Atmospheric fluxes of LSOP contributed by 7% to LDOP pool and could sustain up to 8% of the heterotrophic prokaryotic phosphate demand in the SML of the NW Mediterranean Sea during the stratification period. The results obtained in this study stress the need to include atmospheric fluxes of organic matter in marine biogeochemical models to achieve a more complete picture of carbon and nutrient cycle in the Mediterranean Sea.



**Keywords:** atmospheric deposition, organic carbon, organic nitrogen, organic phosphate, C:N:P ratios, dissolved organic matter, Mediterranean Sea.


## 1. Introduction

The oligotrophic regions cover a significant portion of the global ocean (60%) [Eppley and Peterson, 1979]. These areas are characterized by low concentrations of surface nutrients because of strong stratification and low upward supply of nutrients. In the surface layer, the pool of dissolved organic matter (DOM) plays an important role in maintaining the biological activity as it's an important source of energy and nutrient [Sandberg et al., 2004]. The concentration of dissolved organic nitrogen (DON) and phosphate (DOP) exceed those of inorganic nutrients by an order of magnitude [Bronk, 2002; Lomas et al., 2010**]** and can serve as nitrogen and phosphate source for microbial growth [Sipler and Bronk, 2015 and references therein; Karl and Björkman, 2015 and references therein]. The seasonal variability of dissolved organic carbon (DOC) in the euphotic zone has been recorded in the subtropical

and temperate areas of the ocean [Carlson et al., 1994; Santinelli et al., 2013]. The lag time between DOC production and consumption, causes DOC accumulation in the upper layers [Carlson et al., 1994; Thingstad et al., 1997; Santinelli et al., 2013]. Part of the DOC which is accumulated in the surface layer is exported to the deep by diffusion and/or due to both deep water formation and winter vertical mixing constituting an important pathway for the export of carbon from the surface to the deep ocean [Letcher and Moore, 2015]. At the global ocean, DOM provides of about 20% of global export production [Hansell et al., 2009]. In addition, the elemental ratios of the DOM pool deviate widely from the Redfield ratio being enriched on C in comparison to N and P which suggests a higher carbon export efficiency compared to particulate organic matter [Church and Ducklow, 2002; Hopkinson and Vallino, 2005].

Accurate quantification of DOM sources is needed to achieve a complete picture of C and nutrient cycle in the oligotrophic ocean. In the open ocean, DOM pool is produced mainly by the biological activity in the euphotic layer [Carlson and Hansell, 2015 and references therein]. The microbial activity has been identified to be involved in recalcitrant DOM (RDOM) generation [Taylor et al., 1985; Brophy and Carlson, 1989; Jiao et al., 2010] which can persist in the ocean for millennia and is therefore a reservoir for carbon storage in the ocean [Jiao et al., 2010, 2014]. Besides local production, external sources may contribute significantly to the DOM pool. River flux from land to ocean is an important source of DOM to marine environment, at the scale of the global ocean [Meybeck, 1982] and of the Mediterranean Sea [Ludwig et al., 2009; Panagiotopoulos et al., 2012; Ferreto et al., 2017]. In open waters, where there is little riverine input, groundwater discharge or sediment resuspension, atmospheric deposition becomes a significant source of elements to the surface ocean [Jickells et al., 2005]. However, to date, most measurements of atmospheric deposition to the open ocean have focused on the inorganic fraction [e.g. Duce et al., 1991; Zhang et al., 2010; Guieu et al., 2014] and data on atmospheric fluxes of organic matter to the open ocean are scarce [e.g. Kanakidou et al., 2012] biasing our knowledge on the biogeochemical role of atmospheric deposition in the surface ocean. And yet, the quantification of the atmospheric flux of organic matter could be important since the anthropic emissions of N and P have been enhanced greatly by demographic growth, industrialization, and agricultural intensification. Anthropogenic reactive nitrogen production including inorganic reduced forms of nitrogen (e.g. $NH_3$, $NH_4^+$), inorganic oxidized forms (e.g. $NO_x$, $HNO_3$, $N_2O$, $NO_3$) and organic compounds (e.g. urea, amines, proteins, nucleic acids) could reach 270 T g N $yr^{-1}$ in 2050 [Galloway et al., 2004]. Similarly, P mobilization rose from about 50 Mt P $yr^{-1}$ in preindustrial time to 155 Mt P $yr^{-1}$ in 2000 [Smil, 2000]. In that context of increasing anthropic emissions in the atmosphere, including variable components of organic matter, it seems important to assess how atmospheric organic matter fluxes could influence the biogeochemistry of DOM in ocean surface waters with consequences on carbon export.

The Mediterranean Sea is an oceanic basin representative of an enclosed mini-ocean. Its own conveyer belt and fast circulation times compared to open ocean make it highly reactive to external forcing particularly matter fluxes at the interfaces [Mermex group, 2011 and references therein]. The Mediterranean Sea is of oligotrophic character due, among others, to a pronounced thermal stratification occurring especially during the summer period which

delimits a depleted nutrients surface layer from the deeper [Moutin and Raimbault, 2002; Pulido-Villena et al., 2010]. During the stratification period, both autotrophic and heterotrophic prokaryotic activities are P-limited [Thingstad et al., 1998; Van Wambeke et al., 2002]. Nutrient limitation has been hypothesized to enhance DOC accumulation during the stratification period in the Mediterranean Sea [Thingstad et al., 1997]. In this oceanic region, DOC fluxes play a crucial role in the supply of fresh carbon to the deep water [Ramondenec et al., 2016] both through vertical winter mixing and deep-water formation. In situ measurements estimate that DOC export fluxes are greater or similar than the mean export of POC [Santinelli, 2015 and references therein]. Similarly, a recent modelling study based on varying C:P quotas of planktonic cells, estimated that DOC is responsible of 64% and 90% of the carbon export in the western and eastern Mediterranean basin, respectively [Guyennon et al., 2015]. The Mediterranean Sea is subjected to continuous atmospheric fluxes of anthropogenic sources. Moreover, it receives a noticeable flux of dust from arid regions of North Africa, in the form of strong pulses [Guerzoni et al., 1999], as well as seasonal inputs from biomass burning [Mermex group, 2011 and references therein]. The supply of new nutrients to the Mediterranean Sea from atmospheric deposition and their impact on the activity of phytoplankton and heterotrophic prokaryotes have been extensively addressed [Ridame and Guieu, 2002; Pulido-Villena et al., 2008; Marin et al., 2017]. In contrast, little attention has been paid to the organic fraction of atmospheric deposition precluding the evaluation of its biogeochemical role in the Mediterranean Sea [e.g. Pulido-Villena et al., 2008; Markaki et al., 2010; Sanchez-Pérez et al., 2016].

The aims of this study were to quantify atmospheric fluxes of soluble organic carbon (SOC), nitrogen (SON), and phosphate (SOP) and to estimate the relative contribution of this external source to the inventory of the surface DOC, DON and DOP pools in the NW Mediterranean Sea during the stratification period. For this purpose, we coupled field observations of atmospheric deposition of SOC, SON, and SOP and of DOC, DON and DOP dynamics in the marine surface layer.

# 2. Material and Methods

## 2.1. Atmospheric deposition sampling

Bulk atmospheric deposition (dry plus wet deposition) was sampled twice a month at Frioul Island (43.26° N 05.29° E) in Marseille Bay in the NW Mediterranean Sea (Fig. 1) from February 2015 to July 2016. The collector was set up on a cliff at 40 m above sea level and consisted on an open funnel (314 $cm^2$) connected to a sampling HDPE bottle (2 L) with a nylon membrane (40 µm) in the neck of the funnel preventing contamination from plants, debris and insects. The height of the collector was 2 m above the ground level. Prior to sampling, the collector was cleaned with 10% hydrochloric acid solution and ultrapure water. Every sampling day, the collector was recovered and transferred to the laboratory in a clean plastic bag. Under a laminar flow hood, the inner walls of the funnel were rinsed with 100 mL of ultrapure water after having removed debris deposited on the nylon membrane by means of a plastic clamp. The volume of the rainfall was then determined by the difference in the weight of the sampling bottle before and after sampling to which the volume of ultrapure water added to rinse the funnel was subtracted. If the sample volume collected was less than

600 mL (volume needed to perform all analysis), this one was made up to 600 mL with ultrapure water. Two hundred mL were filtered through a pre-weighed GF/F filter for the determination of particulate matter content as dry weight (60°C, 24h). The remaining volume (400 mL) was filtered through a pre-cleaned (10% HCl + ultrapure water) 0.2 µm polycarbonate filter for chemical analyses.

### 2.2. Seawater sampling

Seawater was sampled monthly between April 2015 to June 2016 on board the *R / V Tethys II* at the permanent time series MOOSE ANTARES offshore station (42.81° N, 6.79° E). Due to unfavorable weather conditions, samplings on November 2015 and between January and March 2016 could not be conducted. Seawater samples were collected at 4 to 7 depths between the surface and 200 m from the Niskin bottles for dissolved organic carbon (DOC), dissolved organic nitrogen (DON), dissolved organic phosphate (DOP), labile dissolved organic phosphorus (LDOP), heterotrophic prokaryotic abundance (HPA), heterotrophic prokaryotic production (HPP), and community respiration (CR). Data on in situ temperature, salinity, oxygen concentrations, and fluorescence were also collected from a SeaBird CTD. For DOM measurements, seawater samples were filtered on board through pre-cleaned (10 % HCl + ultrapure water) 0.2 µm pore size polycarbonate filters and were kept frozen until analysis. Samples were collected in duplicate into acid washed HDPE 60 mL bottles.

For heterotrophic prokaryotic abundance (HPA), heterotrophic prokaryotic production (HPP) and community respiration (CR) unfiltered seawater was sampled. For HPA, duplicate subsamples (1.8 mL) were collected, fixed with 200 µl of paraformaldehyde (20 %), kept at ambient temperature for 15 min, placed in the freezer (-20 °C) available on board, and then stored at -80 °C in the laboratory until analysis. For CR, samples were siphoned directly from the Niskin bottle into eight oxygen bottles. Four bottles from each depth were immediately fixed with Winkler reagents, and the remaining bottles were incubated 24 h in the dark in a tap water bath to minimize temperature variation.

### 2.3. Analytical methods

DOC was measured using a Shimadzu (Model TOC-V total) carbon analyzer with a quartz combustion column filled with 1.2% Pt on silica pillows (Sempéré et al., 2008). Prior to analysis, samples were acidified with a few drops of orthophosphoric acid ($H_3PO_4$, 85%). The daily calibration curve was based on 5 (0, 50, 100, 150 and 300 µM) and 4 (0, 50, 100 and 150 µM) standard solutions of potassium acid phthalate (1000 ng $L^{-1}$) for atmospheric SOC and marine DOC, respectively. One hundred µl of sample were injected between 3 and 5 times for each sample and standard. The analytical precision of the procedure, based on 3 to 5 injection and analyses of the same sample, was 1.5% on average. The accuracy of the instrument and the system blank were determined by analyzing reference materials (D. Hansell, Rosenstiel School of Marine and Atmospheric Science, Miami, USA), including the Deep Seawater reference (DSR) and low carbon water (LCW) reference materials. The average DOC concentrations in the DSR and LCW reference standards were 45 ± 2 µM C, n= 24 and 1 ± 0.3 µM C, n= 24, respectively. Batch number references were Batch#15, Lot#01-15 for DSR and Lot#12-01-B2 for LCW.

DON and DOP concentrations were estimated from the difference between two determinations of dissolved inorganic nitrogen (DIN) and phosphate (SRP for soluble reactive phosphate). The first determination took place after hydrolysis of the sample (total dissolved nitrogen and phosphate, TDN and TDP) and the second one on non- hydrolyzed sample (DIN and SRP). DIN and TDN in both atmospheric and marine samples were analyzed by continuous flow according to Aminot and Kerouel (2007) using a Technicon autoanalyser with an estimated accuracy of 20 nM. TDN was analyzed after persulfate wet-oxidation [Pujo-Pay et al., 1997]. For atmospheric samples, SRP and TDP were analyzed spectrophotometrically on a 10-cm cell after Murphy and Riley (1962) method. TDP was obtained after UV digestion [Armstrong et al., 1966]. For marine samples, due to low concentrations expected, SRP and TDP were analyzed spectrophotometrically by using a long waveguide capillary cell (LWCC) according to Pulido-Villena et al. (2010). The LWCC was 2.5 m long and the limit of detection, estimated as three times the standard deviation of 10 measurements of the blank was 0.8 nM. The labile fraction of DOP in marine (LDOP) and atmospheric samples (LSOP) was obtained after an enzymatic hydrolysis with alkaline phosphatase (AP) from *Esherichia Coli* [Feuillade and Dorioz., 1992; Suzumura et al., 2012; Hashihama et al., 2013]. The AP was diluted with pure water to prepare a working AP solution of 0.2 U $mL^{-1}$. Equal volumes (0.6 mL) of AP working solution and Tris buffer (0.5 M) were added to 30 mL of the sample. Samples were incubated during 3 hours in the dark at a temperature between 25 and 30 °C before phosphate concentration analysis. The duration of the incubation was checked with glucose 6-phosphate in the same conditions of the sample to determine if this duration was sufficient to achieve the whole DOP hydrolysis. To assess any contamination, phosphate concentration was measured in 30 mL of milli-Q water in which 0.6 mL of working AP and Tris buffer were introduced.

Heterotrophic prokaryotic abundance (HPA) counts were performed by cytometry with a FACSCalibur at the MIO-PRECYM flow cytometry platform. Heterotrophic prokaryotic cells were stained with SYBR Green II (Molecular Probes) 1:10 diluted for 15 minutes in the dark at ambient temperature, and were detected by their signature in a plot of side scatter (SCC) versus FLI (green fluorescence). Cells were characterized by 2 main optical signals collected from the 488 nm laser: side scatter (SSC, related to cell structure) and green fluorescence (530/488 nm), related to nucleic acids staining. Regions were established on the SSC versus green fluorescence plot in order to discriminate cells with high nucleic acid (HNA) content from cells with low nucleic acid (LNA) content. Abundance of heterotrophic prokaryotic cells were determined for each subgroup.

Heterotrophic prokaryotic production (HPP) was estimated using the $^{3}$H-leucine incorporation method [Kirchman et al., 1993], adapted with the centrifuge method [Smith and Azam, 1992]. Triplicate aliquots of 1.5 mL were taken for each depth plus one trichloacetic acid (TCA, 5% final) control. The Leucine tracer was used at 20 nM final concentration (with a mix of 14 nM hot leucine (L-[$^{3}$H] leucine, Perkin Elmer® specific activity 106 Ci $mmol^{-1}$) and 6 nM cold leucine) in incubation lasting 2 hours in the dark. The incorporation of Leucine was stopped with the addition of TCA (5% final concentration), then, they were kept at - 4°C until analysis (within few days). After three runs of centrifugation/aspiration of the

supernatant (once with the fixed sea water sample, once with a 5 % TCA rinse, once with an 80 % ethanol rinse), the pellet was resuspended in Scintillation liquid. We used the standard conversion factors of 1.5 kg C mol Leu$^{-1}$ [Kirchman et al., 1993], assuming no isotopic dilution as checked occasionally from concentration kinetics.

Community respiration (CR) was determined from the decrease in oxygen concentration before and after incubation. $O_2$ concentrations were measured following the Winkler method [Carrit and Carpenter, 1966] and a respiratory quotient of 1 [Del Giorgio and Cole, 1998] was applied to convert to C units. A minimum and maximum value of heterotrophic prokaryotic respiration (HPR) was estimated by multiplying the CR by 33% and 78% which represent the range of the contribution of HPR to CR in the NW Mediterranean Sea [Lemée et al., 2002].

### 2.4. Experimental assessment of atmospheric SOC bioavailability

The bioavailability of atmospheric SOC was experimentally assessed on one sample of atmospheric deposition collected on April 2016 during a Saharan dust event. A natural inoculum of marine heterotrophic prokaryotes was added to sterile filtered rainwater. The rainwater sample was filtered through 0.2 µm and adjusted to a marine salinity of 35 using precombusted (450°C, 6 hours) NaCl cristals. A concentrated inoculum of marine heterotrophic prokaryotes was prepared using surface marine water (5 m) collected at the MOOSE ANTARES offshore site, which was subsequently filtered on board through a 40 µm mesh plankton and then by a 0.8 µm Nuclepore polycarbonate filter. Finally, the heterotrophic prokaryotes were concentrated 15 times from 1.5 L of the < 0.8 µm filtrate using a 0.2 µm Nuclepore polycarbonate filter. At the end of the filtration, a volume of 100 mL of the supernatant was recovered with the 0.2 µm filter and was sonicated during 5 mn in order to recover heterotrophic prokaryotes attached to the filter. The objective of this concentration approach was to limit the amount of DOC added with the inoculum which allowed setting the DOC contained in rainwater as the main C source in the incubations. HPA and HPP of the inoculum were 1.6 x $10^6$ cells mL$^{-1}$ and 126 ng C L$^{-1}$ h$^{-1}$, respectively, indicating that the procedure did not seem to affect the vitality of the heterotrophic prokaryote community. Controls consisted of ultrapure water adjusted to a salinity of 35 in which the same inoculum of heterotrophic prokaryotes were added. The experimental bottles were incubated in the dark at controlled temperature during 11 days. The experiment was run in triplicate. Subsamples were taken at selected times during the incubation for the determination of HPA, HPP and DOC.

The percentage of the labile SOC (LSOC) was calculated as:

$$LSOC\ (\%) = \frac{[SOC]_{initial} - [SOC]_{final}}{[SOC]_{initial}}\, x\ 100.$$

### 2.5. Calculations

#### 2.5.1. Air-mass back trajectories

Five-day air-mass back trajectories were calculated at 500, 1000 and 3000 m asl for each sampling date using the Hybrid Single-Particle Lagrangian Integrated Trajectories (HYSPLIT) trajectory model (Draxler and G. Rolph, 2003, NOAA Air Resources Laboratory,

Silver Spring, Maryland, available at http://www.arl.noaa.gov/ready/hysplit4.html) provided by the NOAA Air Resources Laboratory (ARL).

### 2.5.2. Heterotrophic prokaryotic phosphate demand (HPPD)

HPPD, i.e. the phosphate channeled through the heterotrophic prokaryotes, was estimated by dividing the heterotrophic prokaryotic production (HPP) by the C:P ratio of heterotrophic prokaryotic biomass provided in the literature for natural environments. A conservative range of C:P ratios, between 29 (minimum value reported for oceanic bacteria in nature, Cotner et al. 1997 and references therein) and 106 was used for this calculation.

For sampling dates lacking HPP measurements (between April and August 2015), HPP was estimated from HPR (derived from CR) and heterotrophic prokaryotic growth efficiency (HPGE). HPGE (%) was calculated for each sampling date where both HPP and HPR data were available (Sep., Oct. and Dec. 2015, and from Apr. to Jun. 2016) as, $HPP/(HPP + HPR)\ x\ 100$. For each sampling date, a minimum and maximum value of HPGE was estimated corresponding to the minimum and maximum HPR calculated from measured CR. Average $HPGE_{min}$ was 4.7 ± 3.3% and average $HPGE_{max}$ was 10.2 ± 6.5%.

### 2.5.3. Inventories in the surface mixed layer

The mixed layer depth for the marine sampling dates (running from April 2015 to June 2016) was determined following De Boyer Montegut et al. (2004) according to the depth profiles of potential density and temperature. DOC, DON, DOP and biological inventories were calculated for depth intervals in the MLD by vertical trapezoidal integration assuming that the concentration at 0 m is the same as at 5 m:

$$\int_{z1}^{z2} f(x) = (z2 - z1)\ [(f(z1) + f(z2))/2]$$

## 3. Results

### 3.1. Atmospheric fluxes of soluble organic matter (SOM)

Between April 2015 and July 2016, atmospheric fluxes of soluble organic carbon (SOC) ranged between 32 and 588 µmol C $m^{-2}$ $day^{-1}$ (Fig. 2A). Atmospheric fluxes of soluble organic nitrogen (SON) ranged between 7 and 367 µmol N $m^{-2}$ $day^{-1}$ (Fig. 2B) and of soluble organic phosphorus (SOP) between 0.01 and 0.59 µmol P $m^{-2}$ $day^{-1}$ (Fig. 2C). The contribution of the organic fraction to the total soluble fluxes of nitrogen and phosphate ranged between 12 and 83% (41 ± 14%) and between 4 and 57% (25 ± 14%), respectively. The maximum atmospheric flux of soluble organic matter (SOM) was recorded during April and May 2015 when 23% of both SOC and SON and 39% of SOP was deposited. During the rest of the time-series, atmospheric fluxes of SOM were more homogeneous. Considering the entire study period (n = 33), atmospheric fluxes of SOM were significantly related to precipitation rates ($r = 0.43$, $p < 0.01$ for SOC, $r = 0.66$, $p < 0.001$ for SON and $r = 0.38$, $p < 0.05$ for SOP). No significant correlations were observed between atmospheric fluxes of SOM and the atmospheric flux of particulate matter.

### 3.2. Bioavailability of soluble organic phosphate and carbon in atmospheric deposition

The atmospheric flux of labile soluble organic phosphate (LSOP) ranged from 0 to 0.28 µmol $m^{-2}$ $day^{-1}$ over the study period. The contribution of LSOP to the atmospheric flux of SOP showed an important variation during the study period, ranging from 0 to 97% (44 ± 27%).

The labile fraction of soluble organic carbon (LSOC) in atmospheric deposition was estimated only once, through a biodegradation experiment made on a rainwater sample collected in April 2016 (see Material and Methods). In the control treatment, the concentration of DOC at the beginning of the incubations was 7 µM and it remained constant during the 11-day incubation. The heterotrophic prokaryote abundance (HPA) decreased over the experiment and heterotrophic prokaryotic production (HPP) did not exceed 0.35 ng C $L^{-1}$ $h^{-1}$. In the rainwater treatment, the concentration of DOC at the beginning of the incubations was 62 µM and it decreased by 18 ± 3 µM in eleven days which leads to a labile fraction of 29% at this time-scale. During the incubation period, HPA and HPP in the rainwater treatment increased by 6.6 ± 3.3 x $10^5$ cells $mL^{-1}$ and 221 ± 17 ng C $L^{-1}$ $h^{-1}$ respectively.

### 3.3. Dissolved organic matter (DOM) and heterotrophic prokaryotes in the surface layer

#### 3.3.1. Depth profiles

Vertical profiles of DOC, dissolved organic nutrients (DON, DOP and LDOP), dissolved inorganic nutrients (DIN and SRP) and biological activity (HPA, HPP and CR) for all sampling dates are reported in figures S1 to S6. DOC concentration ranged between 39 µM (June 2015 at 200 m) to 86 µM (June 2015 at 5 m). Overall, the depth profiles of DOC were similar during the study period, presenting a slight decrease from the surface to 200 m (Fig. S1). The depth profiles of DON and DOP presented quasi-constant concentrations between the surface and 200 m. DON concentration ranged from 1 µM (August 2015 at 200 m) to a maximum of 10 µM (July 2015) (Fig. S2). DOP concentration ranged between 24 nM (April 2016 at 5 m) to 130 nM (August 2015 at 200 m) (Fig. S3). LDOP ranged between 0 and 34 nM with maximum values observed above the pycnocline decreasing with depth to reach minimal values at 200 m (Fig. S3). In contrast to DON and DOP, DIN and soluble reactive phosphate (SRP) were low above the pycnocline, ranging from the detection limit to 0.34 µM for DIN and between 2 and 47 nM for SRP. Concentrations increased with depth and reached the highest values (8 µM for DIN and 300 nM for SRP) at 200 m (Fig. S4).

The abundance of heterotrophic prokaryotes (HPA) ranged between 3 and 18 x $10^5$ cells $mL^{-1}$ throughout the study period (Fig. S5). The community respiration (CR) ranged from non-detectable values to 0.5 µmol $O_2$ $Kg^{-1}$ $day^{-1}$ (Fig. S5). Heterotrophic prokaryotic production (HPP) data are available only from September 2015 and ranged from undetectable values to 46 ng C $L^{-1}$ $h^{-1}$ (Fig. S6). Both HPA, HPP and CR showed higher values in surface waters and a general decrease with depth.

#### 3.3.2. Depth-integrated inventories

The integrated inventories DOC (mol $m^{-2}$), DON (mol $m^{-2}$), DOP and LDOP (mmol $m^{-2}$) in the surface mixed layer (SML) displayed similar trends during the marine sampling dates with maximum inventories observed in December 2015 (Fig. 3). Over the study period,

SML inventories of DOC ranged between 1.0 and 2.3 mol $m^{-2}$ (Fig. 3A). SML inventories of DON and DOP ranged between 0 and 0.2 mol $m^{-2}$ (Fig. 3B) and between 0.5 and 2.1 mmol $m^{-2}$ (Fig. 3C), respectively. DON and DOP contributed of 98 ± 2% and of 85 ± 11% for TDN and TDP in the SML over the study period, respectively. Inventories of LDOP ranged between 0.14 and 1.02 mmol $m^{-2}$ in the SML (Fig. 3C) and, on average, contributed by 27 ± 19% to the DOP pool.

### 3.4. C:N:P molar ratios in atmospheric SOM and marine DOM

C:N molar ratios in atmospheric soluble organic matter (SOM) ranged between 1.6 and 10.5 (Fig. 4A) with an average value of 5.2 ± 2.3. Marine DOM showed higher C:N ratios, ranging from 2 to 43 with an average of 13.8 ± 6.5. C:P ratios in atmospheric SOM ranged between 352 and 4 200 with an average of 1 228 ± 849. Marine DOM C:P ratios were generally of the same order of magnitude ranging from 326 to 2 850 with an average of 1 227 ± 538 except for August and December 2015 when the C:P ratio was higher in atmospheric deposition (Fig. 4B). N:P ratios in atmospheric SOM ranged between 55 to 2 013 with an average value of 308 ± 349 and a maximum observed during October 2015. Marine DOM N:P ratios were generally lower than in atmospheric SOM and evolved between 9 and 376 with an average value of 100 ± 55 (Fig. 4C).

## 4. Discussion

### 4.1. Atmospheric fluxes

Very few data on atmospheric fluxes of SOC have been reported for the Mediterranean Sea, in particular using frequent deposition data collected over at least one year [Pulido-Villena et al., 2008; De Vicente et al., 2012]. The annual atmospheric flux of SOC obtained in this study (59 mmol $m^{-2}$ $year^{-1}$) is slightly lower than reported in the Ligurian Sea (Cap Ferrat site 129 mmol $m^{-2}$ $year^{-1}$) [Pulido-Villena et al., 2008] and in the southern Spain [De Vicente et al., 2012]. Annual atmospheric flux of SOC in our study is higher than the atmospheric flux (through dry deposition) estimated from the concentration of organic carbon in aerosols collected in the Eastern Mediterranean Sea (Finokalia site: 15 mmol $m^{-2}$ $year^{-1}$) [Theodosi et al., this issue]. The literature on atmospheric fluxes of SON and SOP to the Mediterranean basin is also very limited. The annual atmospheric flux of SOP obtained in this study (69 µmol P $m^{-2}$ $year^{-1}$) is slightly higher than that reported by Migon and Sandroni (1999) (32 µmol P $m^{-2}$ $year^{-1}$) and lower than reported by Violaki et al. (this issue) (1160 and 940 µmol P $m^{-2}$ $year^{-1}$ for the western and eastern basin, respectively). The average contributions of SON and SOP to the total soluble nitrogen and phosphate (TSN, TSP) over the study period were 40% and 25%, respectively. The contribution of SON to TSN in our study was higher than that previously observed by Markaki et al. (2010) while the contribution of SOP to TSP was lower than those reported in the Mediterranean basin [Markaki et al., 2010; Violaki et al., this issue]. Anyhow, given the few existing data, it is difficult to conclude if the observed differences reflect a spatial or inter-annual variability or if they are caused by differences in the sampling protocols and analytical methods.

To our knowledge, there are no reported measurements of atmospheric fluxes of SOC, SON and SOP simultaneously, a single modelling study quantified these atmospheric fluxes

at the global ocean scale [Kanakidou et al., 2012]. For the first time, in this study, coupled atmospheric fluxes of SOC, SON and SOP were quantified in the NW Mediterranean Sea. Over the study period, atmospheric fluxes of SOC, SON and SOP were significantly inter-correlated suggesting a common source and similar transport patterns. The atmospheric fluxes of SOC, SON and SOP were significantly correlated with precipitation rates indicating a high efficiency in atmospheric deposition of SOM via rain events in the NW Mediterranean Sea. These rain events occurred in 80% of our sampling dates and showed important amplitude of variability (between 0.4 and 47 mm). Hereafter, to get further insight on factors controlling the observed atmospheric fluxes of SOM, we have discriminated sampling dates presenting precipitation rates higher than 10 mm from the rest of sampling. Precipitation rates higher than 10 mm were recorded in 8 out of 33 sampling dates. In these samples, differences in SOM atmospheric fluxes observed may be attributable to the differences in rain amount. The maximum atmospheric flux of soluble organic matter was observed during the rain event of April 2015 (Fig. 2) and coincided with a maximum precipitation rate (47 mm during 15 days). This agrees with the observations by Pan et al. (2010) who reported high atmospheric fluxes of SOC coinciding with important rain events in Northern China. However, two other rainfall events of the same magnitude (32 and 37 mm during 15 days) were not accompanied by such a significant atmospheric flux of SOM, suggesting that other factors than rain amount controlled the magnitude of atmospheric flux of SOM in the study area. Back trajectories showed air masses coming from the North for the rain event of April 2015 whereas they came from the West and East during the rainfall of September 2015 and from the South with a Saharan influence for the rainfall of April 2016. These observations suggest that the maximum atmospheric fluxes of SOC, SON and SOP in the NW Mediterranean Sea result from a combination of an anthropogenic influence and an important precipitation rate. Indeed, anthropogenic emissions are known to enhance the presence of organic aerosols in the atmosphere [Kanakidou et al., 2000; 2005; Sempéré and Kawamura, 2003]. In the opposite, the minimum atmospheric flux of SOC, SON and SOP coincided with the rain event of April 2016, suggesting that atmospheric fluxes with a desert signature are poorly enriched in soluble organic matter. This observation contrasts with Pulido-Villena et al. (2008) who reported a maximum atmospheric flux of dissolved organic carbon coinciding with a Saharan dust event. The Saharan dust event reported in Pulido-Villena et al. (2008) delivered a much higher particle flux (215 mg $m^{-2}$ $day^{-1}$) than that reported in our study (5.2 mg $m^{-2}$ $day^{-1}$). The high SOC flux observed by Pulido-Villena et al. (2008) was perhaps a result of heterogeneous reactions between organic compounds and mineral dust in the troposphere (Usher et al. 2003 and references therein).

### 4.2. Marine dissolved organic matter (DOM)

To date, technical limitations have dramatically constrained the data coverage on DOP concentration in surface waters of the Mediterranean Sea. Indeed, the quantitative estimation of DOP relies upon an accurate measurement of SRP concentration, which is below the detection limit given by the conventional colorimetric method (20 nM) in the surface layer during most part of the year [Moutin and Raimbault, 2002; Pulido-Villena et al., 2010]. In this study, an alternative high sensitive SRP analysis method, involving the Long Wave Guide Capillary Cell (LWCC), was applied allowing to get accurate measurements of SRP

concentration and, thus, of DOP in the NW Mediterranean area. Therefore, this study provides the first complete dataset on the temporal variation of DOC, DON, DOP and LDOP concentration in surface waters of the NW Mediterranean Sea.

DOC concentrations obtained over the study period are consistent with values reported for surface waters of the NW Mediterranean Sea [Avril, 2002; Pujo-Pay et al., 2011] as well as for the other parts of the Mediterranean Sea [Sempéré et al, 2002; 2003; Pujo-Pay et al., 2011; Santinelli et al., 2012]. Likewise, DON concentrations reported in this study are in good agreement with previously reported data in the Mediterranean Sea [Diaz et al., 2001; Pujo-Pay et al., 2011]. DOP concentrations above the pycnocline ranged between 25 and 78 nM with an average of 52 nM compared to few nanomoles of SRP. These concentrations compare well with DOP concentrations measured in the Eastern Mediterranean Sea using the same technology [Krom et al., 2005]. LDOP concentrations were in the same range as SRP concentrations in upper waters. However, the increase of SRP concentration below the pycnocline was not accompanied by an increase of the LDOP concentration in agreement with the observations by Hashihama et al. (2013) in the oligotrophic western North Pacific and East China Sea. This suggests that LDOP was still actively hydrolyzed below the pycnocline despite the high concentration of SRP. The elevated DOC concentrations in the upper waters and the slight decrease observed with increasing depth could suggest a net accumulation of carbon in the surface layer. The net accumulation of organic carbon is the difference between sources and sinks which are mainly attributed to biological processes in the marine environments. Phytoplankton activity and their grazer's or viruses activity are considered as the main primary DOM sources in the euphotic layer [Carlson and Hansell, 2015 and reference therein)]. The quasi-constant DON and DOP profile between the surface and 200 m observed in our study, could suggest a balance between production/consumption and import/export processes of both DON and DOP.

Concerning the integrated DOM inventories in the SML (Fig. 3), DOC, DON and DOP followed the same trend over the study period suggesting a control through common processes. The maximum integrated inventories were observed during December 2015 which suggests an accumulation at the end of the stratification period (Fig.3A, B and C). DON and DOP contributions to the TDN and TDP are important in the SML over the study period and are in good agreement with reported literature data in the Mediterranean Sea [Moutin and Raimbault, 2002; Santinelli et al., 2012]. The labile fraction of DOP (LDOP) also contributed significantly (27 ± 19%) to the SML DOP pool over the study period. This contribution was higher than that observed in the oligotrophic Western Pacific and Eastern China (12 ± 7%) [Haschiama et al., 2013].Contrarily to DOP, LDOP did not accumulate at the end of the stratification period and could therefore sustain the autotrophic and heterotrophic activity in the P-depleted uppers waters of the NW Mediterranean Sea.

### 4.3. Elemental ratios in both atmospheric SOM and marine DOM

C:N:P ratios of SOM in atmospheric deposition did not show a seasonal pattern, but seemed rather to be related to a punctual dominance of the atmospheric flux of one of the three elements. Except for a few sampling dates, C:N:P ratios displayed relatively constant values. For example, the average C:N ratio was higher between April and September (2015)

(Fig. 4A), linked to the high SOC fluxes. C:N ratios obtained in this study were in good agreement with C:N ratios of water soluble fraction of aerosols reported in both northern and southern Pacific (Sempéré and Kawamura, 2003). At the opposite, for C:P ratios, two sampling date deviates from the mean (Fig. 4B) but in this case linked to very low fluxes of SOP rather than deviations in SOC flux. Finally, the N:P ratio showed two maximum values linked to the lowest fluxes of SOP (Fig. 4C). The N:P ratios were, in average, higher in the organic fraction (308 ± 349) than in the inorganic fraction (175 ± 234) and were of the same order of magnitude as previously reported [Krom et al., 2004; Markaki et al., 2010].

The precise quantification of DOP concentration above 2 nM using the LWCC technique, allowed assessing for the first time the temporal variability in elemental C:N:P ratios of DOM above the pycnocline in the NW Mediterranean Sea. C:N, C:P and N:P showed average values over the study period of 13 ± 3, 1 430 ± 410 and 112 ± 47, respectively, without any seasonal trend. Elemental ratios of marine DOM showed different values, in average, than atmospheric deposition of SOM. Indeed, C:N ratios of marine DOM were somewhat higher than in atmospheric SOM while N:P ratios were higher in atmospheric deposition due to high atmospheric fluxes of SON. The lack of signature of atmospheric deposition in C:N:P ratios of marine DOM could suggest a quick transformation of atmospheric SOM in the upper waters. C:N:P ratios in atmospheric deposition may thus affect C:N:P ratios in DOM above the pycnocline, but it is difficult to establish a direct link on one year of data. The incorporation of the data obtained in this study into ocean biogeochemical models would certainly help to get further insight on the contribution of atmospheric deposition on elemental ratios of DOM.

### 4.4. Potential biogeochemical implications of atmospheric fluxes of SOM

Assuming ranges obtained in this study for atmospheric fluxes valid for the whole western Mediterranean Sea, annual atmospheric fluxes of SOC, SON and SOP represent 0.2%, 1.2% and 0.5% of modelled atmospheric flux of SOM at the global ocean scale (Kanakidou et al., 2012, Table 1). A comparison with the major input fluxes of DOM to the Western Mediterranean Sea (rivers and straits) highlights that annual atmospheric fluxes of carbon can account for 20 to 25% of the net inputs trough Gibraltar and Sicily straits while annual atmospheric fluxes of nitrogen are in the same order of magnitude. Annual atmospheric flux of organic phosphate was lower than straits net inputs, accounting between 1 and 3% of them (Table 1). In comparison to the Rhône river, which is the most affluent river in the Mediterranean Sea, atmospheric fluxes of SOC, SON and SOP were higher than DOC, DON and DOP fluxes delivered from that river by a factor of 6, 17 and 2 respectively (Table 1). These results highlight the need of accounting for atmospheric inputs, particularly in biogeochemical models, in order to achieve an accurate budget of DOM in the Mediterranean Sea.

One of the key points of our study is the simultaneous survey of atmospheric SOM fluxes and marine DOM inventories which provides a direct quantification of the contribution of the atmospheric SOM deposition to surface DOM pool. In this study, we choose to quantify this contribution over the period from April 2015 to October 2015 which corresponds to the stratification period, when the surface mixed layer (SML) was isolated

from the deep layers making the atmospheric deposition a major source. The contribution of atmospheric SOM to the DOM pool in the SML during that period was calculated by dividing the atmospheric cumulative integrated flux (Table 3) by the surface mixed layer DOM inventories (Table 2) during that period. The contribution of atmospheric deposition of SOM to the DOM pool during that period in the surface layer of the NW Mediterranean Sea were low for SOC (3%), SOP (4.5%) and moderate for LSOP (7%) and SON (12%) (Table 3).

A better understanding of the role of atmospheric deposition of SOM relies on the knowledge on its bioavailability. Previous studies examining the effects of atmospheric inputs have focused on the inorganic fraction [Maranon et al., 2010; Pulido-Villena et al., 2014; Herut et al., 2016]. The few reported studies on the bioavailability of atmospheric organic matter concerned organic nitrogen [Timperley et al., 1985; Peierls and Paerl, 1997, Seitzinger and Sanders, 1999; Seitzinger et al., 2002] and none of these studies took place in the Mediterranean Sea. This study presents the first examination of the bioavailability of atmospheric SOC and SOP to marine heterotrophic prokaryotes, and suggests that a substantial fraction of atmospheric SOC (29% over 11-days period) and SOP (44 ± 27%) would be bioavailable. The quantification of the labile fraction of SOP (LSOP) derived from atmospheric deposition can have important consequences in the P-depleted Mediterranean surface waters since marine heterotrophic prokaryotes could hydrolyze labile DOP to alleviate P stress. Atmospheric LSOP being quantified over the study period, we have assessed its potential contribution to the heterotrophic prokaryotic phosphate demand (HPPD, Table 2), in the SML during the period between April and October 2015 (Table 3). The LSOP: HPPD ratio was calculated by dividing minimal and maximal atmospheric fluxes by minimal and maximal HPPD (Table 3) and suggested low to moderate contributions of LSOP to the heterotrophic prokaryotic phosphate demand (Table 3). The atmospheric LSOC may contribute also to the heterotrophic prokaryotic carbon demand (HPCD). However, to estimate this contribution, the bioavailability of atmospheric samples of different origins at different periods would be necessary.

## 5. Concluding Remarks

This work provides a unique data set of simultaneous atmospheric fluxes of soluble organic matter (SOM) and marine dissolved organic matter (DOM) inventories in the NW Mediterranean Sea and leads to the following major conclusions: (1) A substantial fraction of atmospheric deposition of nitrogen and phosphate to the Mediterranean Sea is in the form of soluble organic matter accounting of 40% and 25%, respectively. (2) In the surface mixed layer, DOP contributed by 85 ± 11% to TDP with 27 ± 19% of the DOP pool as LDOP. (3) Atmospheric deposition is a significant source of soluble organic matter to upper waters of the western Mediterranean Sea, greater than river input. (4) The direct contribution of atmospheric deposition of SOM to surface DOM pool is low to moderate although further research on its bioavailability is needed to understand its biogeochemical role in the NW Mediterranean Sea. Overall, the results obtained in this study highlight the need of incorporating atmospheric fluxes of SOM into biogeochemical models to better constrain the DOM cycle in upper waters in oligotrophic regions such as the Mediterranean Sea.

**Acknowledgments**

This work is a contribution to the Labex OT-Med (n° ANR-11-LABX-0061) funded by the French Government «Investissements d'Avenir» program of the French National Research Agency (ANR) through the A*MIDEX project (n° ANR-11-IDEX-0001-02). This study was conducted as part of the WP4 MERMEX/MISTRALS project and is a contribution to the international SOLAS, IMBER and LOICZ programs. We would like to thank the MOOSE project for the help in accessing the atmospheric and marine sampling sites, the captain and the crew of R/V Tethys II for their cooperative work at sea, PRECYM flow cytometry platform and Michel Fournier for the valuable assistance provided during the installation of the collector of atmospheric bulk deposition.

## References

Aminot, A., Kérouel, R., 2004. Dissolved organic carbon, nitrogen and phosphorus in the N-E Atlantic and the N-W Mediterranean with particular reference to non-refractory fractions and degradation. *Deep Sea Research Part I: Oceanographic Research Papers*, 51, 1975-1999.

Aminot, A., Kérouel., R., 2007. Dosage automatique des nutriments dans les eaux marines: méthodes en flux continu. *Ed. Ifremer,méthode d'analyse en milieu marin*, 188 p.

Armstrong, F.A.J., Williams, P.M., Strickland, J.D.H., 1966. Photo-oxidation of Organic Matter in Sea Water by Ultra-violet Radiation, Analytical and Other Applications. *Nature*, 211, 481-483.

Avril, B., 2002. DOC dynamics in the northwestern Mediterranean Sea (DYFAMED site). *Deep-Sea Research Part Ii-Topical Studies in Oceanography*, 49, 2163-2182.

Bronk, D.A. (2002), Dynamics of DON, in Biogeochemistry of Marine Dissolved Organic Matter, 1st ed., edited by D. A. Hansell and C. A. Carlson, pp.153–247, Academic Press, San Diego, CA, doi:10.1016/B978-012323841-2/50007-5

Brophy, J.E., Carlson, D.J., 1989. Production of Biologically Refractory Dissolved Organic-Carbon by Natural Seawater Microbial-Populations. *Deep-Sea Research Part a-Oceanographic Research Papers*, 36, 497-507.

Carlson, C.A., Ducklow, H.W., Michaels, A.F., 1994. Annual flux of dissolved organic-carbon from the euphotic zone in the Northwestern Sargasso Sea. *Nature*, 371, 405-408.

Carlson, C.A., Giovannoni, S.J., Hansell, D.A., Goldberg, S.J., Parsons, R., Otero, M.P., Vergin, K., Wheeler, B.R., 2002. Effect of nutrient amendments on bacterioplankton production, community structure, and DOC utilization in the northwestern Sargasso Sea. *Aquatic Microbial Ecology*, 30, 19-36.

Carlson, CA and Hansell, DA., 2015. DOM Sources, Sinks, Reactivity, and Budgets. In: Dennis A. Hansell and Craig A. Carlson. (Eds.) Biogeochemistry of Marine Dissolved Organic Matter. *Academic Press*. 579-608.

Carritt, D.E., Carpenter, J., 1966. Comparison and evaluation of currently employed modifications of Winkler method for determining dissolved oxygen in seawater-a NASCO Report. *Journal of Marine Research*, 24.

Church, M.J., Ducklow, H.W., Karl, D.M., 2002. Multiyear increases in dissolved organic matter inventories at Station ALOHA in the North Pacific Subtropical Gyre. *Limnology and Oceanography*, 47, 1-10.

Coste, B., Corre, P.L., Minas, H.J., 1988. Re-evaluation of the nutrient exchanges in the strait of Gibraltar. *Deep Sea Research Part A. Oceanographic Research Papers*, 35, 767-775.

Cotner, J.B., J.W. Ammerman,E. R. Peele, and E. Bentzen, Phosphorus-limited bacterioplankton growth in the Sargasso Sea, *Aquatic Microbial Ecology*, 13 (2), 141–149, 1997.

Craig, A.C., Stephen, J.G., Dennis, A.H., Stuart, J.G., Rachel, P., Mark, P.O., Kevin, V., Benjamin, R.W., 2002. Effect of nutrient amendments on bacterioplankton production, community structure, and DOC utilization in the northwestern Sargasso Sea. *Aquatic Microbial Ecology*, 30, 19-36.

De Boyer Montégut, C., Madec, G., Fischer, A.S., Lazar, A., Iudicone, D., 2004. Mixed layer depth over the global ocean: An examination of profile data and a profile-based climatology. *Journal of Geophysical Research: Oceans*, 109, 1-20.

De Vicente, I., Ortega-Retuerta, E., Morales-Baquero, R., Reche, I., 2012. Contribution of dust inputs to dissolved organic carbon and water transparency in Mediterranean reservoirs. *Biogeosciences*, 9, 5049-5060.

Del Giorgio, P.A., Cole, J.J., 1998. Bacterial growth efficiency in natural aquatic systems. *Annual Review of Ecology and Systematics*, 29, 503-541.

Diaz, F., Raimbault, P., Boudjellal, B., Garcia, N., Moutin, T., 2001. Early spring phosphorus limitation of primary productivity in a NW Mediterranean coastal zone (Gulf of Lions). *Marine Ecology Progress Series*, 211, 51-62.

Duce, R.A., Liss, P.S., Merrill, J.T., Atlas, E.L., Buat-Menard, P., Hicks, B.B., Miller, J.M., Prospero, J.M., Arimoto, R., Church, T.M., Ellis, W., Galloway, J.N., Hansen, L., Jickells, T.D., Knap, A.H., Reinhardt, K.H., Schneider, B., Soudine, A., Tokos, J.J., Tsunogai, S., Wollast, R., Zhou, M., 1991. The atmospheric input of trace species to the world ocean. *Global Biogeochemical Cycles*, 5, 193-259.

Eppley, R.W., Peterson, B.J., 1979. Particulate Organic-Matter Flux and Planktonic New Production in the Deep Ocean. *Nature*, 282, 677-680.

Ferretto, N., Tedetti, M., Guigue, C., Mounier, S., Raimbault, P., Goutx, M., 2017. Spatio-temporal variability of fluorescent dissolved organic matter in the Rhne River delta and the Fos-Marseille marine area (NW Mediterranean Sea, France). *Environmental Science and Pollution Research*, 24, 4973-4989.

Feuillade, M., Dorioz, J.M., 1992. Enzymatic release of phosphate in sediments of various origins. *Water Research*, 26, 1195-1201.

Galloway, J.N., Dentener, F.J., Capone, D.G., Boyer, E.W., Howarth, R.W., Seitzinger, S.P., Asner, G.P., Cleveland, C.C., Green, P.A., Holland, E.A., Karl, D.M., Michaels, A.F., Porter, J.H., Townsend, A.R., Vöosmarty, C.J., 2004. Nitrogen Cycles: Past, Present, and Future. *Biogeochemistry*, 70, 153-226.

Gruber, D.F., Simjouw, J.P., Seitzinger, S.P., Taghon, G.L., 2006. Dynamics and characterization of refractory dissolved organic matter produced by a pure bacterial culture in an experimental predator-prey system. *Applied and Environmental Microbiology*, 72, 4184-4191.

Guerzoni, S., Chester, R., Dulac, F., Herut, B., Loye-Pilot, M.D., Measures, C., Migon, C., Molinaroli, E., Moulin, C., Rossini, P., Saydam, C., Soudine, A., Ziveri, P., 1999. The

role of atmospheric deposition in the biogeochemistry of the Mediterranean Sea. *Progress in Oceanography*, 44, 147-190.

Guieu, C., Aumont, O., Paytan, A., Bopp, L., Law, C.S., Mahowald, N., Achterberg, E.P., Maranon, E., Salihoglu, B., Crise, A., Wagener, T., Herut, B., Desboeufs, K., Kanakidou, M., Olgun, N., Peters, F., Pulido-Villena, E., Tovar-Sanchez, A., Volker, C., 2014. The significance of the episodic nature of atmospheric deposition to Low Nutrient Low Chlorophyll regions. *Global Biogeochemical Cycles*, 28, 1179-1198.

Guyennon, A., Baklouti, M., Diaz, F., Palmieri, J., Beuvier, J., Lebaupin-Brossier, C., Arsouze, T., Beranger, K., Dutay, J.C., Moutin, T., 2015. New insights into the organic carbon export in the Mediterranean Sea from 3-D modeling. *Biogeosciences*, 12, 7025-7046.

Hansell, D.A., 2013. Recalcitrant Dissolved Organic Carbon Fractions. In C.A. Carlson, S.J. Giovannoni (Eds.), *Annual Review of Marine Science, Vol 5*, Vol. 5 (pp. 421-445). Palo Alto: Annual Reviews.

Hashihama, F., Kinouchi, S., Suwa, S., Suzumura, M., Kanda, J., 2013. Sensitive determination of enzymatically labile dissolved organic phosphorus and its vertical profiles in the oligotrophic western North Pacific and East China Sea. *Journal of Oceanography*, 69, 357-367.

Herut, B., Rahav, E., Tsagaraki, T.M., Giannakourou, A., Tsiola, A., Psarra, S., Lagaria, A., Papageorgiou, N., Mihalopoulos, N., Theodosi, C.N., Violaki, K., Stathopoulou, E., Scoullos, M., Krom, M.D., Stockdale, A., Shi, Z., Berman-Frank, I., Meador, T.B., Tanaka, T., Paraskevi, P., 2016. The Potential Impact of Saharan Dust and Polluted Aerosols on Microbial Populations in the East Mediterranean Sea, an Overview of a Mesocosm Experimental Approach. *Frontiers in Marine Science*, 3.

Hopkinson, C.S., Vallino, J.J., 2005. Efficient export of carbon to the deep ocean through dissolved organic matter. *Nature*, 433, 142-145.

Jiao, N., Herndl, G.J., Hansell, D.A., Benner, R., Kattner, G., Wilhelm, S.W., Kirchman, D.L., Weinbauer, M.G., Luo, T.W., Chen, F., Azam, F., 2010. Microbial production of recalcitrant dissolved organic matter: long-term carbon storage in the global ocean. *Nature Reviews Microbiology*, 8, 593-599.

Jiao, N., Robinson, C., Azam, F., Thomas, H., Baltar, F., Dang, H., Hardman-Mountford, N.J., Johnson, M., Kirchman, D.L., Koch, B.P., Legendre, L., Li, C., Liu, J., Luo, T., Luo, Y.W., Mitra, A., Romanou, A., Tang, K., Wang, X., Zhang, C., Zhang, R., 2014. Mechanisms of microbial carbon sequestration in the ocean - future research directions. *Biogeosciences*, 11, 5285-5306.

Jickells, T.D., An, Z.S., Andersen, K.K., Baker, A.R., Bergametti, G., Brooks, N., Cao, J.J., Boyd, P.W., Duce, R.A., Hunter, K.A., Kawahata, H., Kubilay, N., laRoche, J., Liss, P.S., Mahowald, N., Prospero, J.M., Ridgwell, A.J., Tegen, I., Torres, R., 2005. Global iron connections between desert Dust, Ocean Biogeochemistry, and Climate. *Science*, 308, 67-71.

Kanakidou, M., Duce, R.A., Prospero, J.M., Baker, A.R., Benitez-Nelson, C., Dentener, F.J., Hunter, K.A., Liss, P.S., Mahowald, N., Okin, G.S., Sarin, M., Tsigaridis, K., Uematsu, M., Zamora, L.M., Zhu, T., 2012. Atmospheric fluxes of organic N and P to the global ocean. *Global Biogeochemical Cycles*, 26.

694 Kanakidou, M., Seinfeld, J.H., Pandis, S.N., Barnes, I., Dentener, F.J., Facchini, M.C., Van
695 Dingenen, R., Ervens, B., Nenes, A., Nielsen, C.J., Swietlicki, E., Putaud, J.P.,
696 Balkanski, Y., Fuzzi, S., Horth, J., Moortgat, G.K., Winterhalter, R., Myhre, C.E.L.,
697 Tsigaridis, K., Vignati, E., Stephanou, E.G., Wilson, J., 2005. Organic aerosol and
698 global climate modelling: a review. *Atmos. Chem. Phys.*, 5, 1053-1123.
699 Kanakidou, M., Tsigaridis, K., Dentener, F.J., Crutzen, P.J., 2000. Human-activity-enhanced
700 formation of organic aerosols by biogenic hydrocarbon oxidation. *Journal of*
701 *Geophysical Research: Atmospheres*, 105, 9243-9354.
702 Karl, DM and Björkman, KM., 2015. Dynamics of Dissolved Organic Phosphorus. In: Dennis
703 A. Hansell and Craig A. Carlson. (Eds.) Biogeochemistry of Marine Dissolved Organic
704 Matter. *Academic Press.* 579-608.
705 Kirchman, D.L., Keil, R.G., Simon, M., Welschmeyer, N.A., 1993. Biomass and Production
706 of Heterotrophic Bacterioplankton in the Oceanic Sub-Arctic Pacific. *Deep-Sea*
707 *Research Part I-Oceanographic Research Papers*, 40, 967-988.
708 Krom, M.D., Herut, B., Mantoura, R.F.C., 2004. Nutrient budget for the Eastern
709 Mediterranean: Implications for phosphorus limitation. *Limnology and Oceanography*,
710 49, 1582-1592.
711 Krom, M.D., Woodward, E.M.S., Herut, B., Kress, N., Carbo, P., Mantoura, R.F.C., Spyres,
712 G., Thingstad, T.F., Wassmann, P., Wexels-Riser, C., Kitidis, V., Law, C.S., Zodiatis,
713 G., 2005. Nutrient cycling in the south east Levantine basin of the eastern
714 Mediterranean: Results from a phosphorus starved system. *Deep-Sea Research Part Ii-*
715 *Topical Studies in Oceanography*, 52, 2879-2896.
716 Laghdass, M., Blain, S., Besseling, M., Catala, P., Guieu, C., Obernosterer, I., 2011. Effects
717 of Saharan dust on the microbial community during a large in situ mesocosm
718 experiment in the NW Mediterranean Sea. *Aquatic Microbial Ecology*, 62, 201-213.
719 Lemee, R., Rochelle-Newall, E., Van Wambeke, F., Pizay, M.D., Rinaldi, P., Gattuso, J.P.,
720 2002. Seasonal variation of bacterial production, respiration and growth efficiency in
721 the open NW Mediterranean Sea (vol 29, pg 227, 2002). *Aquatic Microbial Ecology*,
722 30, 102-102.
723 Letscher, R.T., Moore, J.K., 2015. Preferential remineralization of dissolved organic
724 phosphorus and non-Redfield DOM dynamics in the global ocean: Impacts on marine
725 productivity, nitrogen fixation, and carbon export. *Global Biogeochemical Cycles*, 29,
726 325-340.
727 Lomas, M.W., Steinberg, D.K., Dickey, T., Carlson, C.A., Nelson, N.B., Condon, R.H.,
728 Bates, N.R., 2010. Increased ocean carbon export in the Sargasso Sea linked to climate
729 variability is countered by its enhanced mesopelagic attenuation. *Biogeosciences*, 7, 57-
730 70.
731 Ludwig, W., Dumont, E., Meybeck, M., Heussner, S., 2009. River discharges of water and
732 nutrients to the Mediterranean and Black Sea: Major drivers for ecosystem changes
733 during past and future decades? *Progress in Oceanography*, 80, 199-217.
734 Mahowald, N., Jickells, T.D., Baker, A.R., Artaxo, P., Benitez-Nelson, C.R., Bergametti, G.,
735 Bond, T.C., Chen, Y., Cohen, D.D., Herut, B., Kubilay, N., Losno, R., Luo, C.,
736 Maenhaut, W., McGee, K.A., Okin, G.S., Siefert, R.L., Tsukuda, S., 2008. Global

distribution of atmospheric phosphorus sources, concentrations and deposition rates, and anthropogenic impacts. *Global Biogeochemical Cycles*, 22, n/a-n/a.

Marañon, E., Fernández, A., Mouriño-Carballido, B., MartÍnez-GarcÍa, S., Teira, E., Cermeño, P., Chouciño, P., Huete-Ortega, M., Fernández, E., Calvo-DÍaz, A., Morán, X.A.G., Bode, A., Moreno-Ostos, E., Varela, M.M., Patey, M.D., Achterberg, E.P., 2010. Degree of oligotrophy controls the response of microbial plankton to Saharan dust. *Limnology and Oceanography*, 55, 2339-2352.

Marín, I., Nunes, S., Sánchez-Pérez, E.D., Aparicio, F.L., Estrada, M., Marrasé, C., Moreno, T., Wagener, T., Querol, X., Peters, F., 2017. Anthropogenic versus mineral aerosols in the stimulation of microbial planktonic communities in coastal waters of the northwestern Mediterranean Sea. *Science of The Total Environment*, 574, 553-568.

Markaki, Z., Loye-Pilot, M.D., Violaki, K., Benyahya, L., Mihalopoulos, N., 2010. Variability of atmospheric deposition of dissolved nitrogen and phosphorus in the Mediterranean and possible link to the anomalous seawater N/P ratio. *Marine Chemistry*, 120, 187-194.

Meybeck, M., 1982. Carbon, nitrogen, and phosphorus transport by World Rivers. *American Journal of Science*, 282, 401-450.

Migon, C., Sandroni, V., 1999. Phosphorus in rainwater: Partitioning inputs and impact on the surface coastal ocean. *Limnology and Oceanography*, 44, 1160-1165.

Moutin, T., Raimbault, P., 2002. Primary production, carbon export and nutrients availability in western and eastern Mediterranean Sea in early summer 1996 (MINOS cruise). *Journal of Marine Systems*, 33, 273-288.

Murphy, J., and J. Riley (1962), A modified single solution method for the determination of phosphate in natural waters, Anal. Chim. Acta, 27, 31–36, doi:10.1016/S0003-2670(00)88444-5.

Ogawa, H., Amagai, Y., Koike, I., Kaiser, K., Benner, R., 2001. Production of refractory dissolved organic matter by bacteria. *Science*, 292, 917-920.

Pan, Y., Wang, Y., Xin, J., Tang, G., Song, T., Wang, Y., Li, X., Wu, F., 2010. Study on dissolved organic carbon in precipitation in Northern China. *Atmospheric Environment*, 44, 2350-2357.

Panagiotopoulos, C., Sempere, R., Para, J., Raimbault, P., Rabouille, C., Charriere, B., 2012. The composition and flux of particulate and dissolved carbohydrates from the Rhone River into the Mediterranean Sea. *Biogeosciences*, 9, 1827-1844.

Peierls, B.L., Paerl, H.W., 1997. Bioavailability of atmospheric organic nitrogen deposition to coastal phytoplankton. *Limnology and Oceanography*, 42, 1819-1823.

Pujo-Pay, M., Conan, P., Oriol, L., Cornet-Barthaux, V., Falco, C., Ghiglione, J.F., Goyet, C., Moutin, T., Prieur, L., 2011. Integrated survey of elemental stoichiometry (C, N, P) from the western to eastern Mediterranean Sea. *Biogeosciences*, 8, 883-899.

Pujo-Pay, M., Conan, P., Raimbault, P., 1997. Excretion of dissolved organic nitrogen by phytoplankton assessed by wet oxidation and N-15 tracer procedures. *Marine Ecology Progress Series*, 153, 99-111.

Pulido-Villena, E., Baudoux, A.C., Obernosterer, I., Landa, M., Caparros, J., Catala, P., Georges, C., Harmand, J., Guieu, C., 2014. Microbial food web dynamics in response to

780 a Saharan dust event: results from a mesocosm study in the oligotrophic Mediterranean
781 Sea. *Biogeosciences*, 11, 5607-5619.
782 Pulido-Villena, E., Rerolle, V., Guieu, C., 2010. Transient fertilizing effect of dust in P-
783 deficient LNLC Surface Ocean. *Geophysical Research Letters*, 37, 1-5.
784 Pulido-Villena, E., Wagener, T., Guieu, C., 2008. Bacterial response to dust pulses in the
785 western Mediterranean: Implications for carbon cycling in the oligotrophic ocean.
786 *Global Biogeochemical Cycles*, 22, 1-5.
787 Raimbault, P., Pouvesle, W., Diaz, F., Garcia, N., Sempéré, R., 1999. Wet-oxidation and
788 automated colorimetry for simultaneous determination of organic carbon, nitrogen and
789 phosphorus dissolved in seawater. *Marine Chemistry*, 66, 161-169.
790 Ridame, C., Guieu, C., 2002. Saharan input of phosphate to the oligotrophic water of the open
791 western Mediterranean Sea. *Limnology and Oceanography*, 47, 856-869.
792 Sanchez-Perez, E.D., Marín, I., Nunes, S., Aparicio, F.L., Fernández-González, L., Peters, F.,
793 Pujo-Pay, M., Conan, P., Marrasé, C., 2016. Aerosol inputs affect the optical signatures
794 of dissolved organic matter in NW Mediterranean coastal waters. *Scientia Marina*, 80,
795 437-446.
796 Sandberg, J., Andersson, A., Johansson, S., Wikner, J., 2004. Pelagic food web structure and
797 carbon budget in the northern Baltic Sea: potential importance of terrigenous carbon.
798 *Marine Ecology Progress Series*, 268, 13-29.
799 Santinelli, C., 2015. DOC in the Mediterranean Sea. In: Dennis A. Hansell and Craig A.
800 Carlson (Eds.) Biogeochemistry of Marine Dissolved Organic Matter. *Academic Press.*
801 579-608.
802 Santinelli, C., Ibello, V., Lavezza, R., Civitarese, G., Seritti, A., 2012. New insights into C, N
803 and P stoichiometry in the Mediterranean Sea: The Adriatic Sea case. *Continental Shelf*
804 *Research*, 44, 83-93.
805 Santinelli, C., Hansell, D. A., and d'Alcala M., R. 2013. Influence of stratification on
806 marine dissolved organic carbon (DOC) dynamics: The Mediterranean Sea case, *Prog.*
807 *Oceanogr*., 119, 68–77.
808 Seitzinger, S.P., Sanders, R.W., 1999. Atmospheric inputs of dissolved organic nitrogen
809 stimulate estuarine bacteria and phytoplankton. *Limnology and Oceanography*, 44, 721-
810 730.
811 Seitzinger, S.P., Sanders, R.W., Styles, R., 2002. Bioavailability of DON from natural and
812 anthropogenic sources to estuarine plankton. *Limnology and Oceanography*, 47, 353-
813 366.
814 Sempéré, R., Panagiotopoulos, C., Lafont, R., Marroni, B., Van Wambeke, F., 2002. Total
815 organic carbon dynamics in the Aegean Sea. *Journal of Marine Systems*, 33, 355-364.
816 Sempéré, R., Dafner, E., Van Wambeke, F., Lefèvre, D., Magen, C., Allègre, S., Bruyant, F.,
817 Bianchi, M., Prieur, L., 2003. Distribution and cycling of total organic carbon across the
818 Almeria Oran Front. Biogeochemical implications. Journal of Geophysical Research,
819 108, No. C11, 3361, 10.1029/2002JC001475.
820 Sempéré, R., Kawamura, K., 2003. Trans-hemispheric contribution of C2–C10 α, ω-
821 dicarboxylic acids, and related polar compounds to water-soluble organic carbon in the
822 western Pacific aerosols in relation to photochemical oxidation reactions. *Global*
823 *Biogeochemical Cycles*, 17, 1-14.

Sempéré, R., Tedetti, M., Panagiotopoulos, C., Charrière, B., Van Wambeke, F., 2008. Distribution and bacterial availability of dissolved neutral sugars in the South East Pacific. Biogeosciences Discuss. 5, 725–750. *Doi:*10.5194/bgd-5-725-2008.

Smil, 2000. Phosphorus in the environment: Natural Flows and Human Interferences. *Annual Review of Energy and the Environment*, 25, 53-88.

Smith, D., Farooq, A., 1992. A simple, economical method for measuring bacterial protein synthesis rates in seawater using 3H-leucine 1. *Marine Microbial Food Webs*, 6, 107-114.

Spiller, RE and Bronk, DE., 2015. Dynamics of Dissolved Organic Nitrogen. In: Dennis A. Hansell and Craig A. Carlson. (Eds.) Biogeochemistry of Marine Dissolved Organic Matter. *Academic Press*. 579-608.

Sugimura, Y., Suzuki, Y., 1988. A High-Temperature Catalytic-Oxidation Method for the Determination of Non-Volatile Dissolved Organic-Carbon in Seawater by Direct Injection of a Liquid Sample. *Marine Chemistry*, 24, 105-131.

Suzumura, M., Hashihama, F., Yamada, N., Kinouchi, S., 2012. Dissolved phosphorus pools and alkaline phosphatase activity in the euphotic zone of the western North Pacific Ocean. *Frontiers in Microbiology*, 3.

Taylor, G.T., Iturriaga, R., Sullivan, C.W., 1985. Interactions of Bactivorous Grazers and Heterotrophic Bacteria with Dissolved Organic-Matter. *Marine Ecology Progress Series*, 23, 129-141.

The MERMEX group: Durrieu de Madron, X.D., Guieu, C., Sempere, R., Conan, P., Cossa, D., D'Ortenzio, F., Estournel, C., Gazeau, F., Rabouille, C., Stemmann, L., Bonnet, S., Diaz, F., Koubbi, P., Radakovitch, O., Babin, M., Baklouti, M., Bancon-Montigny, C., Belviso, S., Bensoussan, N., Bonsang, B., Bouloubassi, I., Brunet, C., Cadiou, J.F., Carlotti, F., Chami, M., Charmasson, S., Charriere, B., Dachs, J., Doxaran, D., Dutay, J.C., Elbaz-Poulichet, F., Eleaume, M., Eyrolles, F., Fernandez, C., Fowler, S., Francour, P., Gaertner, J.C., Galzin, R., Gasparini, S., Ghiglione, J.F., Gonzalez, J.L., Goyet, C., Guidi, L., Guizien, K., Heimburger, L.E., Jacquet, S.H.M., Jeffrey, W.H., Joux, F., Le Hir, P., Leblanc, K., Lefevre, D., Lejeusne, C., Leme, R., Loye-Pilot, M.D., Mallet, M., Mejanelle, L., Melin, F., Mellon, C., Merigot, B., Merle, P.L., Migon, C., Miller, W.L., Mortier, L., Mostajir, B., Mousseau, L., Moutin, T., Para, J., Perez, T., Petrenko, A., Poggiale, J.C., Prieur, L., Pujo-Pay, M., Pulido, V., Raimbault, P., Rees, A.P., Ridame, C., Rontani, J.F., Pino, D.R., Sicre, M.A., Taillandier, V., Tamburini, C., Tanaka, T., Taupier-Letage, I., Tedetti, M., Testor, P., Thebault, H., Thouvenin, B., Touratier, F., Tronczynski, J., Ulses, C., Van Wambeke, F., Vantrepotte, V., Vaz, S., Verney, R., MerMex, G., 2011. Marine ecosystems responses to climatic and anthropogenic forcings in the Mediterranean. *Progress in Oceanography*, 91, 97-166.

Theodosi, C., Panagiotopoulos, C., Nouara, A., Zarmpas, P., Nicolaou, P., Violaki, K., Kanakidou, M., Sempéré, R., Mihalopoulos, N., 2017. Sugars in atmospheric aerosols over the Eastern Mediterranean. *This issue*.

Thingstad, T.F., Hagstrom, A., Rassoulzadegan, F., 1997. Accumulation of degradable DOC in surface waters: Is it caused by a malfunctioning microbial loop? *Limnology and Oceanography*, 42, 398-404.

867 Thingstad, T. F., U. L. Zweifel, and F. Rassoulzadegan (1998), P limitation of heterotrophic
868 bacteria and phytoplankton in the northwest Mediterranean, *Limnology and*
869 *Oceanography*, 43, 88– 94.
870 Timperley, M.H., Vigorbrown, R.J., Kawashima, M., Ishigami, M., 1985. Organic Nitrogen-
871 Compounds in Atmospheric Precipitation - Their Chemistry and Availability to
872 Phytoplankton. *Canadian Journal of Fisheries and Aquatic Sciences*, 42, 1171-1177.
873 Usher, C.R., Michel, A.E., Grassian, V.H., 2003. Reactions on mineral dust. *Chem. Rev.*
874 2003, 103, 4883-4939
875 Van Wambeke, F., Christaki, U., Giannokourou, A., Moutin, T., Souvemerzoglou, K., 2002.
876 Longitudinal and vertical trends of bacterial limitation by phosphorus and carbon in the
877 Mediterranean Sea. *Microbial Ecology*, 43, 119-133.
878 Violaki, K., Bourrin, F., Aubert, D., Kouvarakis, G., Delsaut, N., Mihalopoulos, N., 2017.
879 Organic Phosphorus in atmospheric deposition over Mediterranean Sea: An important
880 missing piece of the P cycle. *This issue*.
881 Willey, J.D., Kieber, R.J., Eyman, M.S., Avery, G.B., 2000. Rainwater dissolved organic
882 carbon: Concentrations and global flux. *Global Biogeochemical Cycles*, 14, 139-148.
883 Zhang, Y., Yu, Q., Ma, W.C., Chen, L.M., 2010. Atmospheric deposition of inorganic
884 nitrogen to the eastern China seas and its implications to marine biogeochemistry.
885 *Journal of Geophysical Research-Atmospheres*, 115, 10.
886

## Figure captions

**Figure 1.** Location of the sampling sites: atmospheric deposition at the Frioul Island and sea water sampling at the ANTARES site. Both sampling sites are included in the MOOSE observation network (http://www.moose-network.fr/).

**Figure 2.** Temporal evolution of atmospheric fluxes (µmol $m^{-2}$ $day^{-1}$) of soluble organic carbon (SOC; panel A), total soluble and soluble organic nitrogen (TSN, SON; panel B), total soluble, soluble organic and labile soluble organic phosphate (TSP, SOP, LSOP; panel C), for each 2-week sample collected at the Frioul Island between March 2015 and July 2016. Arrows point to rain events higher than 30 mm. The vertical line differentiates the year 2015 from the year 2016.

**Figure 3.** Integrated inventories of dissolved organic carbon (DOC; panel A), dissolved organic nitrogen (DON; panel B), dissolved organic phosphate and labile dissolved organic phosphate (DOP and LDOP; panel C) in the surface mixed layer over the study period. The mixed layer depth (MLD, m) is also plotted in each panel. The vertical line differentiates the year 2015 from the year 2016.

**Figure 4.** C:N (panel A), C:P (panel B) and N:P (panel C) molar ratios of soluble organic matter in atmospheric deposition (line with squares) and of marine dissolved organic matter between the surface and 200 m depth (box plots: the central mark represents the mean value for all depths, the edges of the box are the 25th and 75th percentiles, the whiskers extend data points to the minimum and the maximum, and the outliers are plotted individually).

**Figure 1**

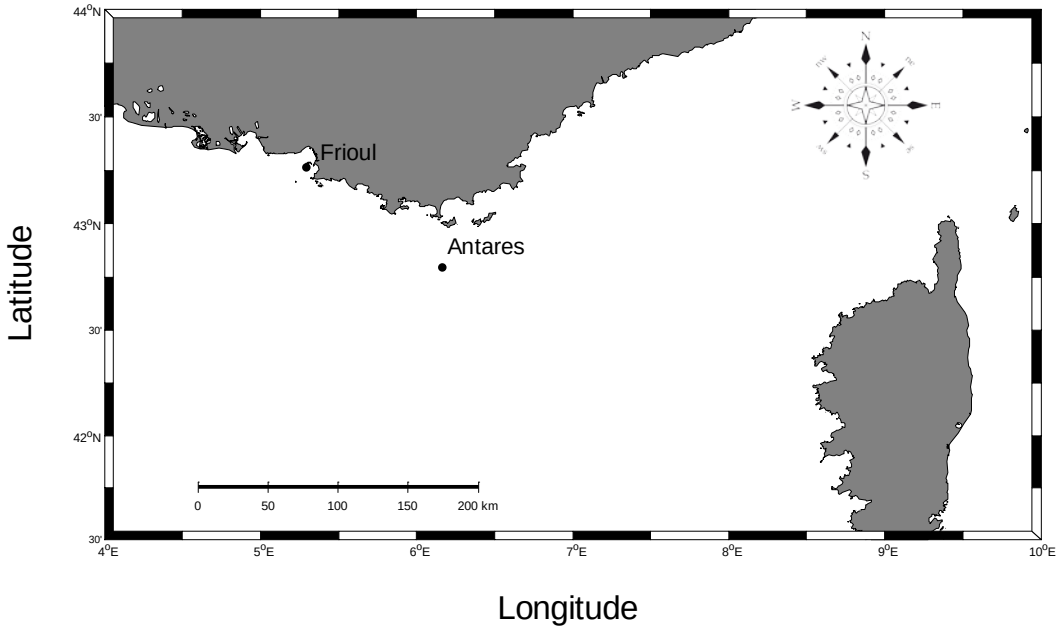


**Figure 2**

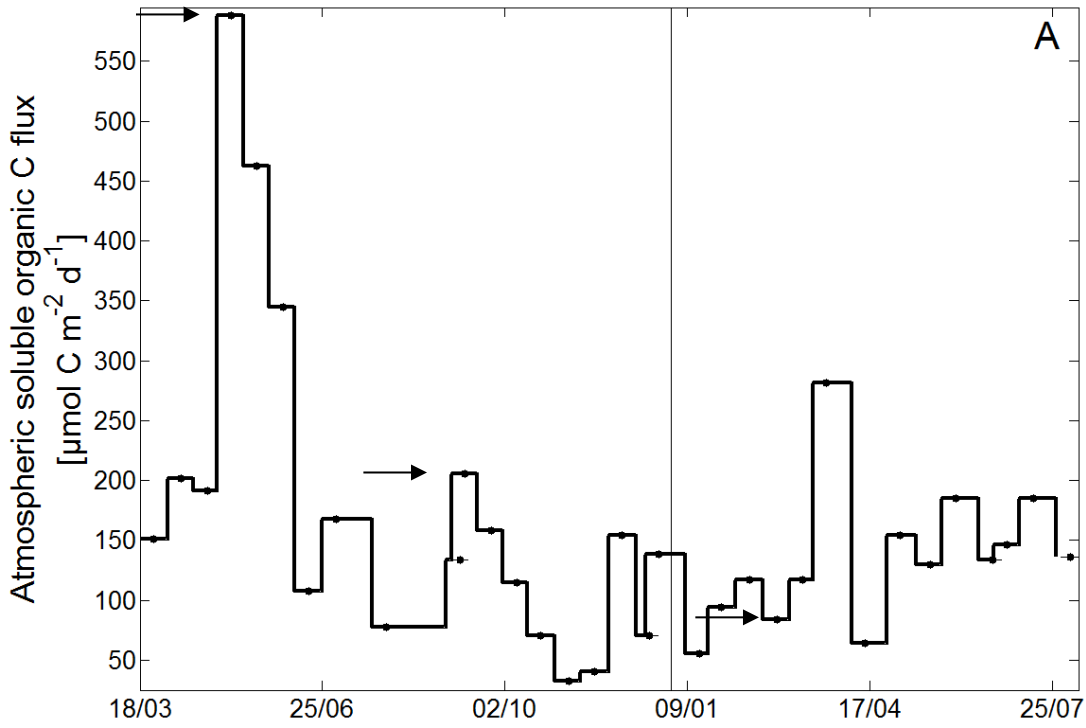

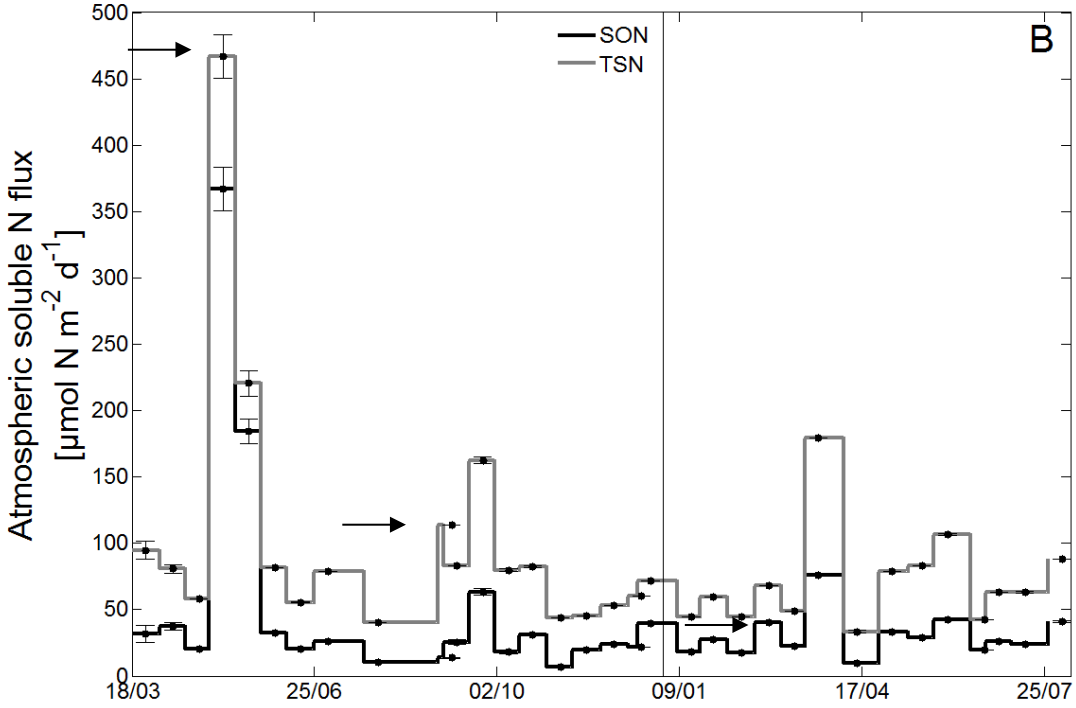


928

929

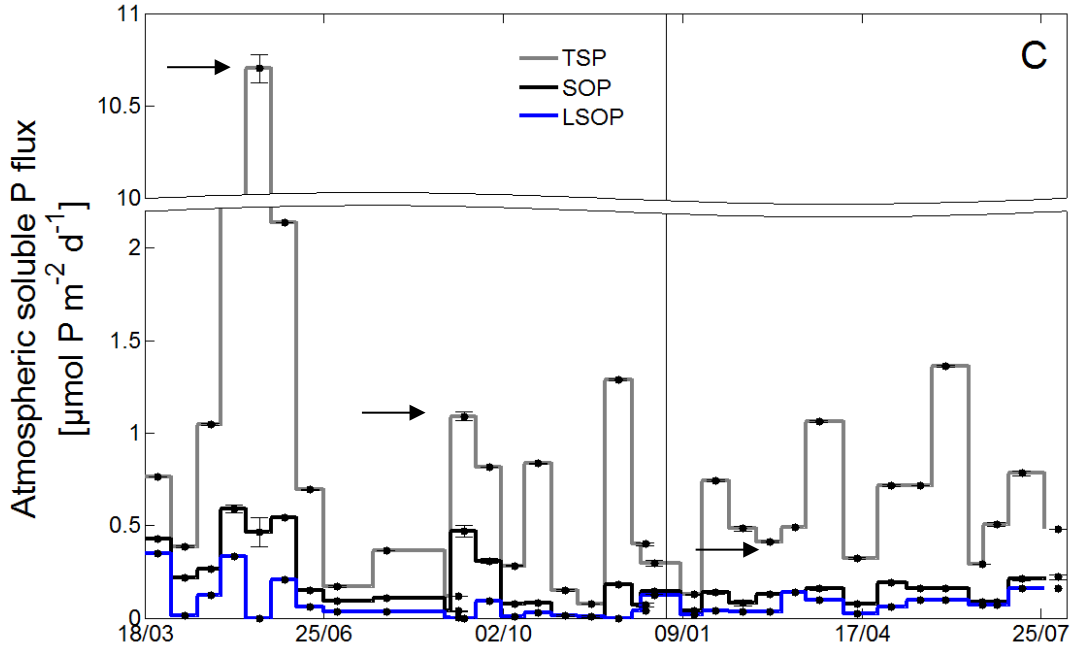


930

931

**Figure 3**

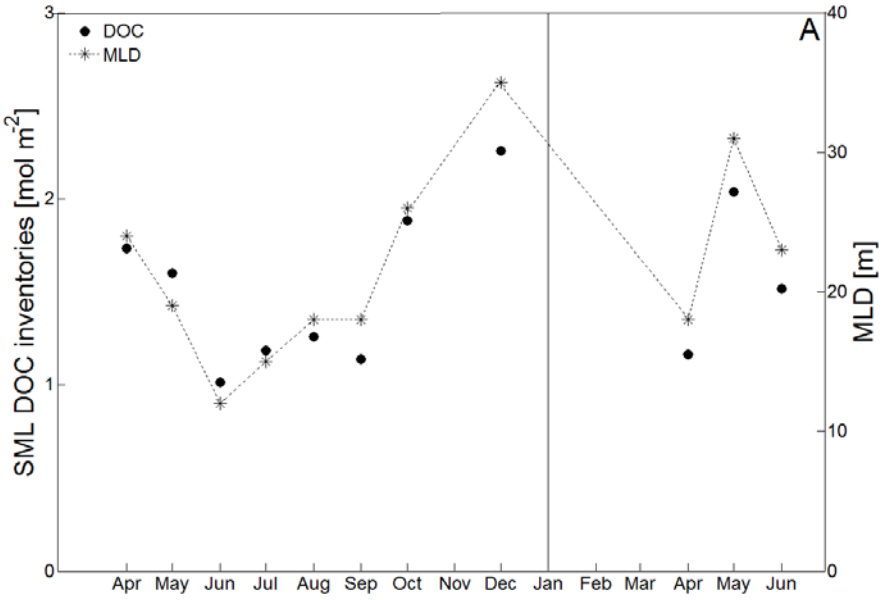
DOC
MLD
A
SML DOC inventories [mol m-2]
MLD [m]
0
1
2
3
0
10
20
30
40
Apr May Jun Jul Aug Sep Oct Nov Dec Jan Feb Mar Apr May Jun

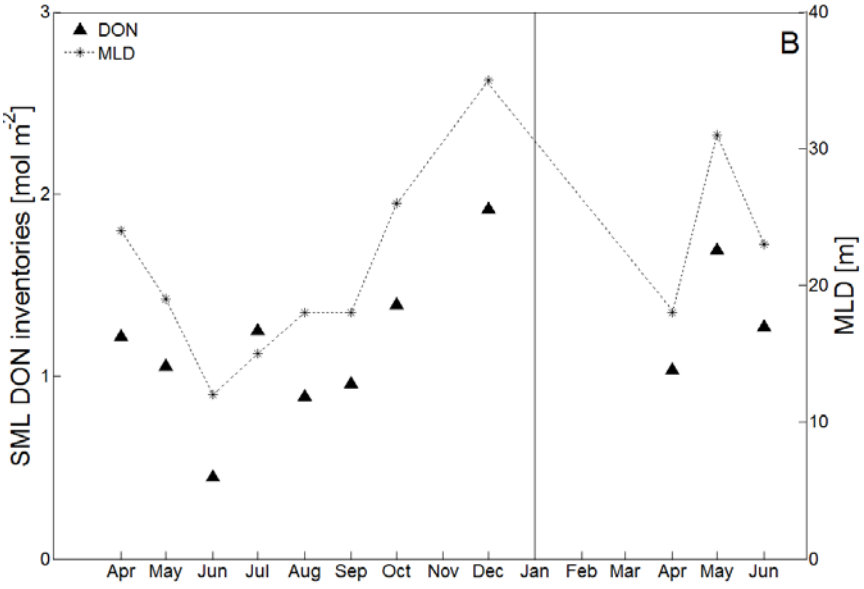
DON
MLD
B
SML DON inventories [mol m-2]
MLD [m]
0
1
2
3
0
10
20
30
40
Apr May Jun Jul Aug Sep Oct Nov Dec Jan Feb Mar Apr May Jun

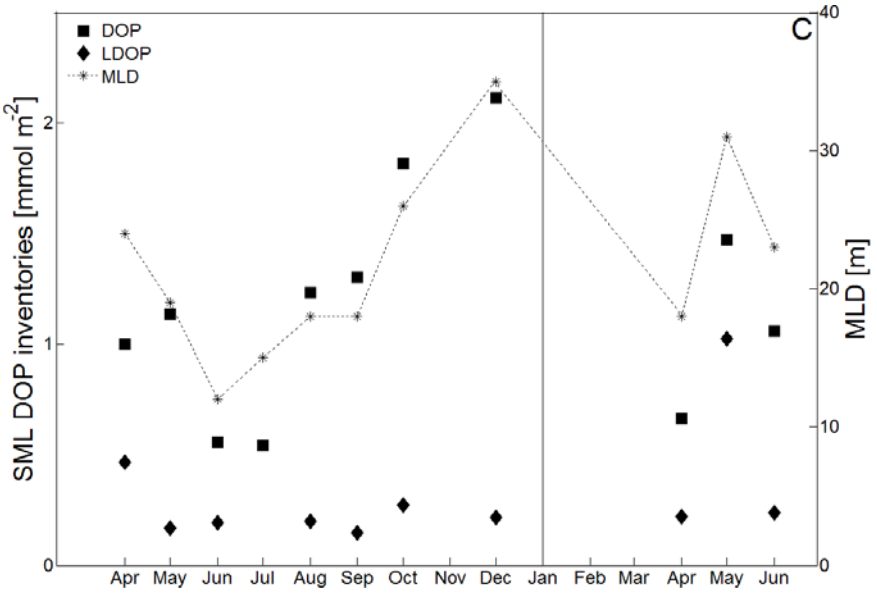


936

937

938

939

940 **Figure 4**

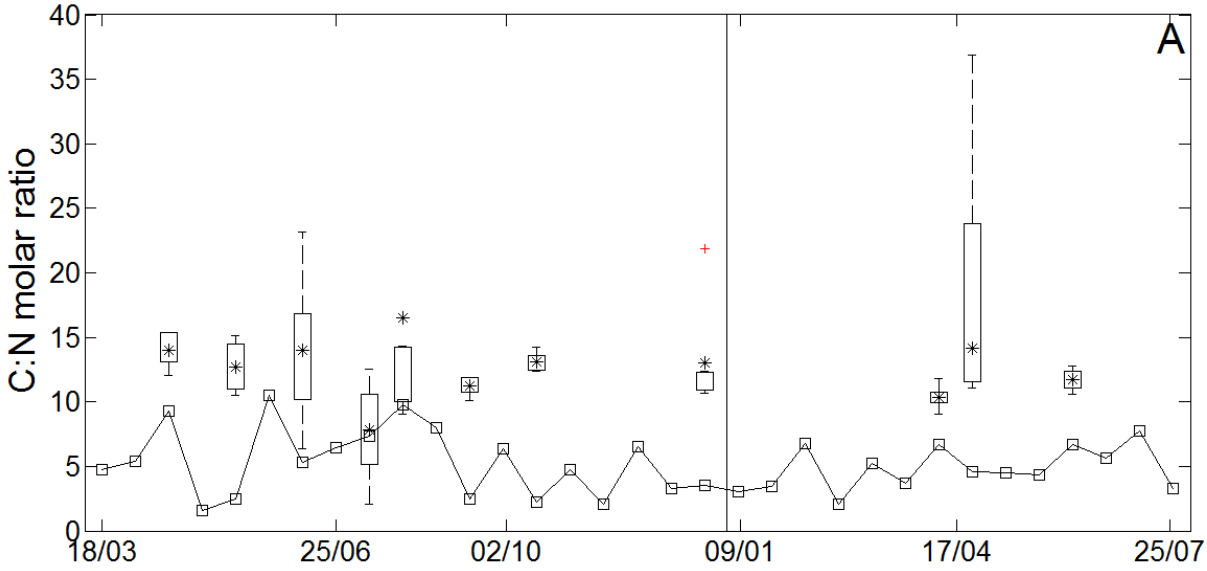


941

942

943

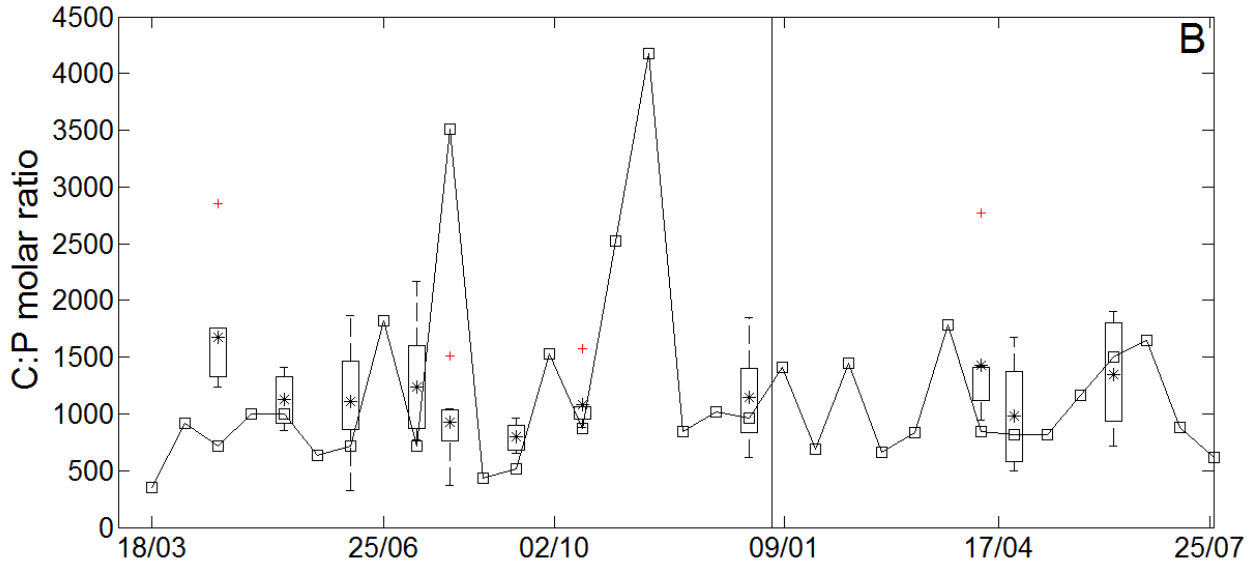


944

945

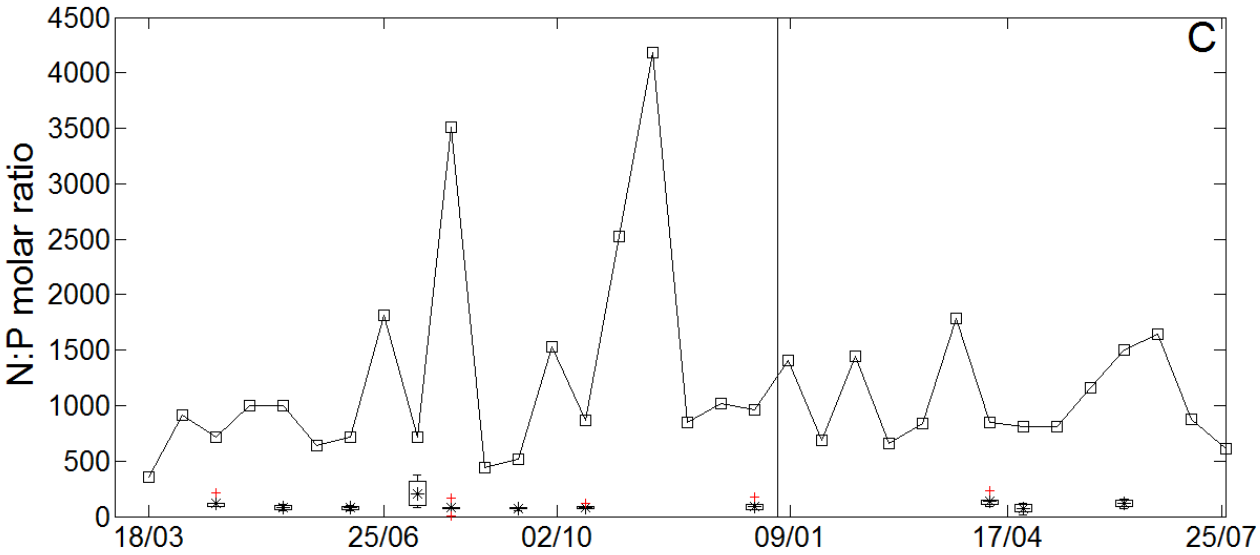


946

947

948

949

950

951

952

953

954

955

**Table 1:** Annual atmospheric fluxes of soluble organic carbon (SOC), soluble organic nitrogen (SON) and soluble organic phosphate (SOP) extrapolated to the western Mediterranean basin compared to dissolved organic carbon (DOC), dissolved organic nitrogen (DON) and dissolved organic phosphate (DOP) fluxes from the Rhône River and net inputs from Sicily and Gibraltar straits.

| | Atmospheric flux[a] | Rhône flux[b] | Global modeled atmospheric flux[c] | Straits net inputs |
|---|---|---|---|---|
| DOC (x $10^{12}$ g C $yr^{-1}$) | 0.595 | 0.104 | 230 | 2.4 - 3.1[d] |
| DON (x $10^{12}$ g N $yr^{-1}$) | 0.193 | 0.011 | 16 | 0.01 - 0.56[e,f] |
| DOP (x $10^{12}$ g P $y^{-1}$) | 0.002 | 0.001 | 0.35 | 0.07 - 0.16[e,f] |

[a]This study, annual atmospheric flux extrapolated to the whole western Mediterranean Sea area (0.84 x $10^6$ $km^2$)

[b]Annual integrated flux (between December 2014 and December 2015) (data courtesy of the MOOSE network:https://doi.org/10.6096/MISTRALS-MOOSE.767 )

[c] From Kanakidou et al (2012)

[d] From Santinelli (2015)

[e] From Pujo-Pay et al (2011)

[f] From Coste et al (1987)

**Table 2:** Depth-integrated inventories (means ± standard deviation) within the surface mixed layer calculated between April and October 2015 (mmol $m^{-2}$). DOM-related inventories: DOC: dissolved organic carbon, DON: dissolved organic nitrogen, DOP: dissolved organic phosphate, LDOP: labile dissolved organic phosphate. Biological activity-related inventories: HPA: heterotrophic prokaryotic abundance, HPP: heterotrophic prokaryotic production, HPR: heterotrophic prokaryotic respiration, HPPD: Heterotrophic prokaryotic phosphate demand. Details on the estimation of HPR and HPPD can be found on the text (sections 2.3 and 2.5, respectively).

| | The stratification period |
|---|---|
| DOM inventories; [mmol $m^{-2}$] | |
| DOC | $(1.4 \pm 0.3) \times 10^3$ |
| DON | $(1 \pm 0.3) \times 10^2$ |
| DOP | $1.1 \pm 0.4$ |
| LDOP | $0.2 \pm 0.1$ |
| Molar ratio | |
| C:N:P | 1360:102:1 |
| Biology inventories | |
| HPA; [cells $m^{-2}$] | $(2.4 \pm 1.2) \times 10^{13}$ |
| HPP; [mmol C $m^{-2}$ $day^{-1}$] | $2.2 \pm 1.5 – 2.3 \pm 1.5$ |
| HPR; [mmol C $m^{-2}$ $day^{-1}$] | $(19.8 \pm 15.1) \times 10^3$ - $(46.7 \pm 35.6) \times 10^3$ |
| HPPD; [mmol P $m^{-2}$ $day^{-1}$] | $(11.4 \pm 8.9) \times 10^{-3} – (55.7 \pm 43.7) \times 10^{-3}$ |

**Table 3:** Cumulative integration of atmospheric fluxes (mmol $m^{-2}$) and molar ratios of soluble organic matter (SOM) for the period between April-02 and October-29 (2015). SOC: soluble organic carbon, SON: soluble organic nitrogen, SOP: soluble organic phosphate, LSOP: labile soluble organic phosphate. Contribution (%) of atmospheric fluxes of SOM to marine surface pool of dissolved organic matter (DOM) and to heterotrophic prokaryotic C and P demand in the mixed layer depth during that period.

*Contributions - related to DOM pool: $C_{DOC}$; contribution of atmospheric SOC to DOC pool, $C_{DON}$; contribution of atmospheric SON to DON pool, $C_{DOP}$; contribution of atmospheric SOP to DOP pool and $C_{LDOP}$; contribution of atmospheric LSOP to LDOP pool.

**Contributions - related to marine heterotrophic prokaryotes: $C_{HPPD}$; contribution of atmospheric LSOP to heterotrophic prokaryotic phosphate demand. Contribution related to marine heterotrophic prokaryotes demand were calculated by using the minimum and the maximum flux of atmospheric labile SOC and SOP observed for each period.

| April-2 to October-29 (2015) cumulative atmospheric flux; [mmol m-2] | |
|---|---|
| SOC | 41.6 |
| SON | 11.9 |
| SOP | $49.2 \times 10^{-3}$ |
| LSOP | $13.6 \times 10^{-3}$ |
| Molar ratio | |
| C:N:P | 841:241:1 |
| Contributions to surface DOM pool; (%)* | |
| $C_{DOC}$ | 3 |
| $C_{DON}$ | 12 |
| $C_{DOP}$ | 4.5 |
| $C_{LDOP}$ | 6.8 |
| Contribution to heterotrophic phosphate demand; (%)** | |
| $C_{HPPD}$ | 0 - 8.6 |

## Supplementary figures

**Figure S1** : Dissolved organic carbon (DOC) vertical depth profiles between the surface and 200 m at the ANTARES station during the study period.

**Figure S2** : Dissolved organic nitrogen (DON) vertical depth profiles between the surface and 200 m at the ANTARES station during the study period.

**Figure S3** : Dissolved organic phosphate (DOP) and labil dissolved organic phosphate (LDOP) vertical depth profiles between the surface and 200 m at the ANTARES station during the study period.

**Figure S4** : Soluble reactive phosphate (SRP) and dissolved inorganic nitrogen (DIN) vertical depth profiles between the surface and 200 m at the ANTARES station during the study period.

**Figure S5**: Heterotrophic prokaryotic abundance (HPA) and community respiration (CR) between the surface and 200 m at the ANTARES station during the study period.

**Figure S6**: Heterotrophic prokaryotic production (HPP) between the surface and 200 m at the ANTARES station during the study period.

**Figure S1**

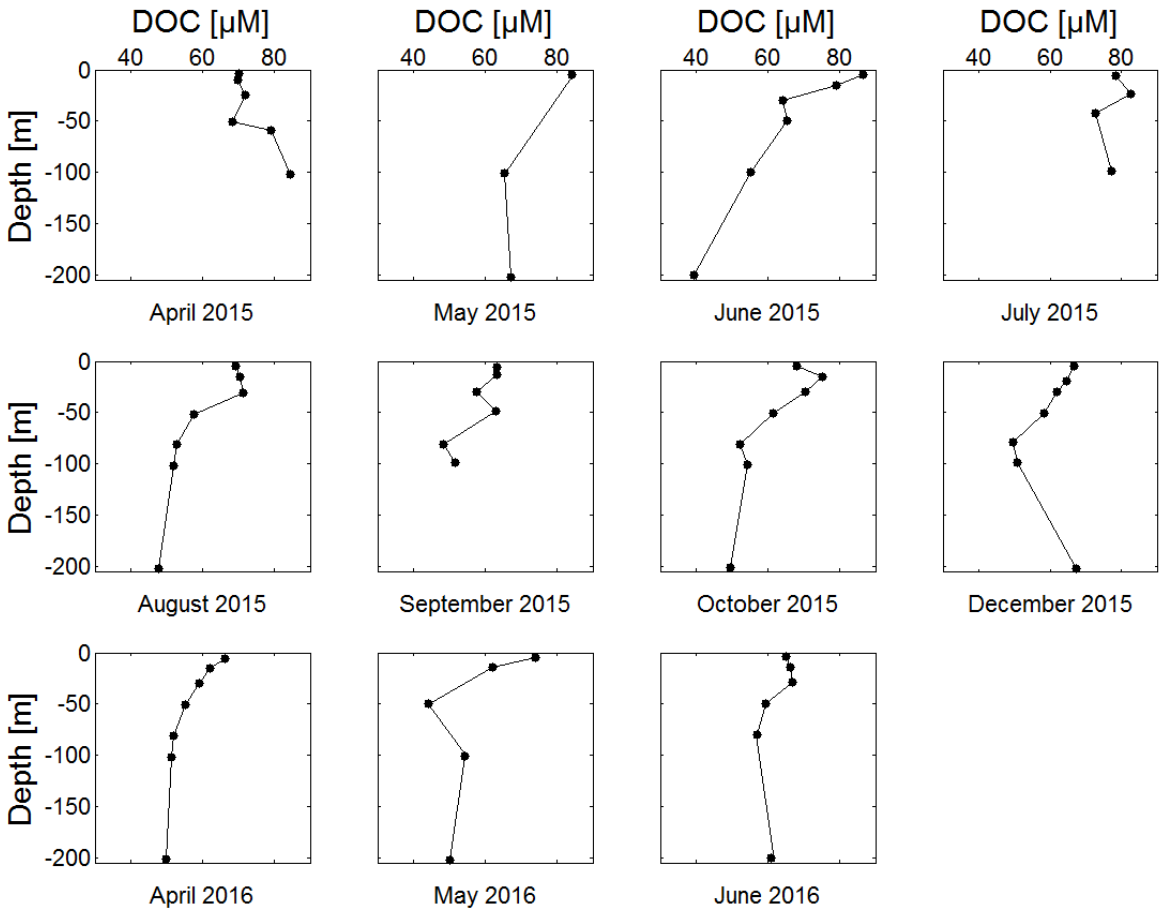
DOC [µM]
40
60
80
Depth [m]
0
-50
-100
-150
-200
April 2015
May 2015
June 2015
July 2015
August 2015
September 2015
October 2015
December 2015
April 2016
May 2016
June 2016

**Figure S2**

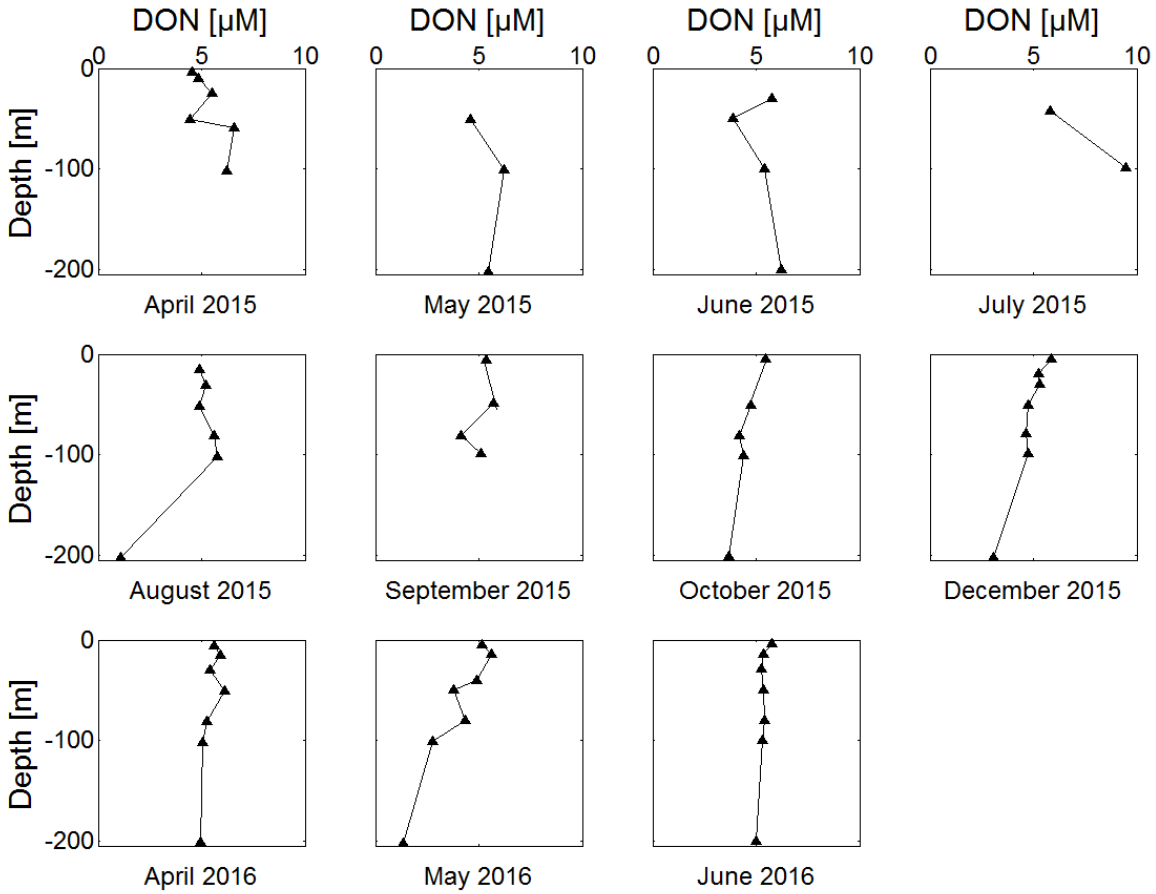
DON [µM]
0
5
10
Depth [m]
-100
-200
April 2015
May 2015
June 2015
July 2015
August 2015
September 2015
October 2015
December 2015
April 2016
May 2016
June 2016

**Figure S3**

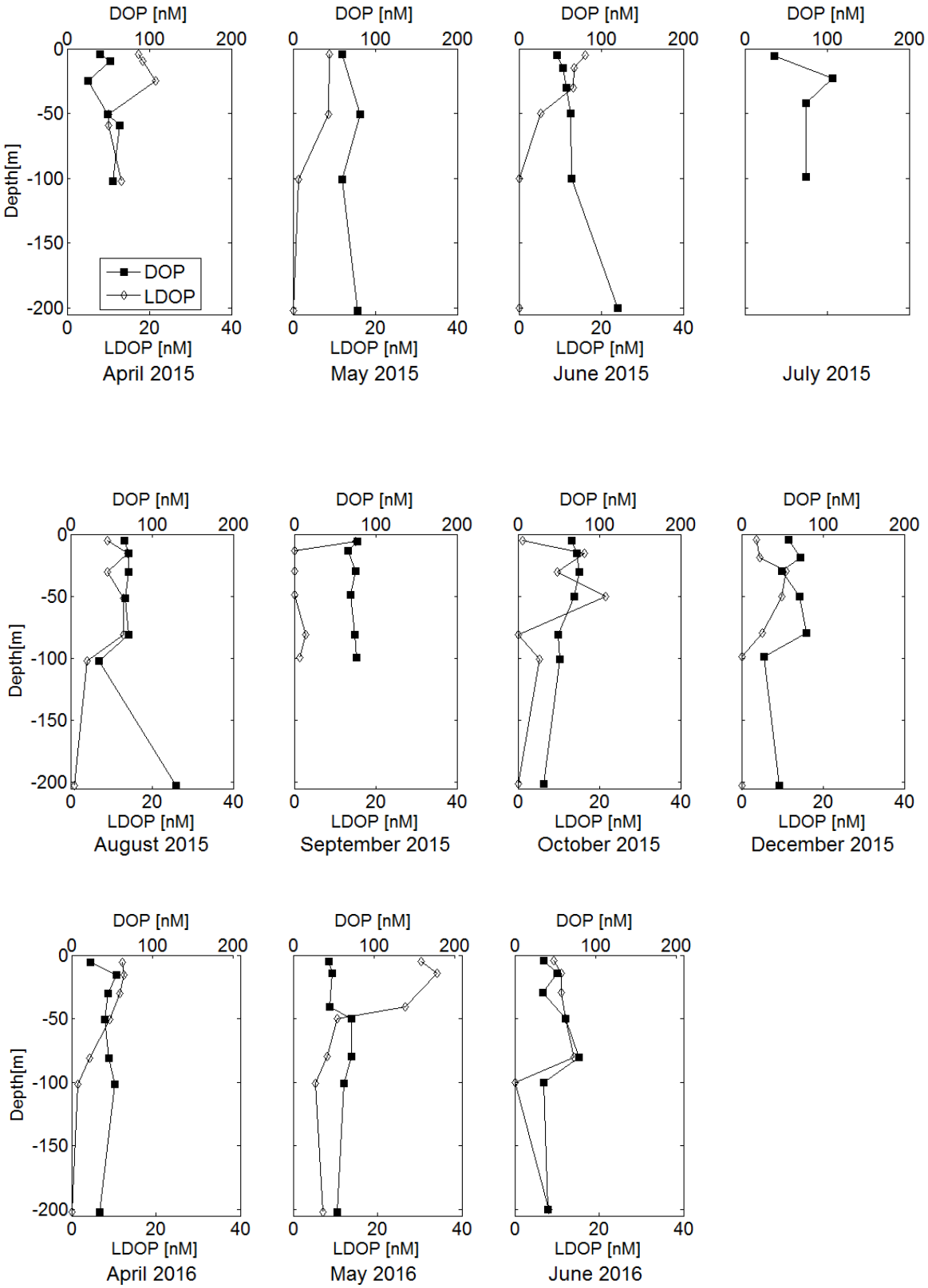
DOP [nM]
0
100
200
Depth[m]
0
-50
-100
-150
-200
DOP
LDOP
0
20
40
LDOP [nM]
April 2015
May 2015
June 2015
July 2015
August 2015
September 2015
October 2015
December 2015
April 2016
May 2016
June 2016

**Figure S4**

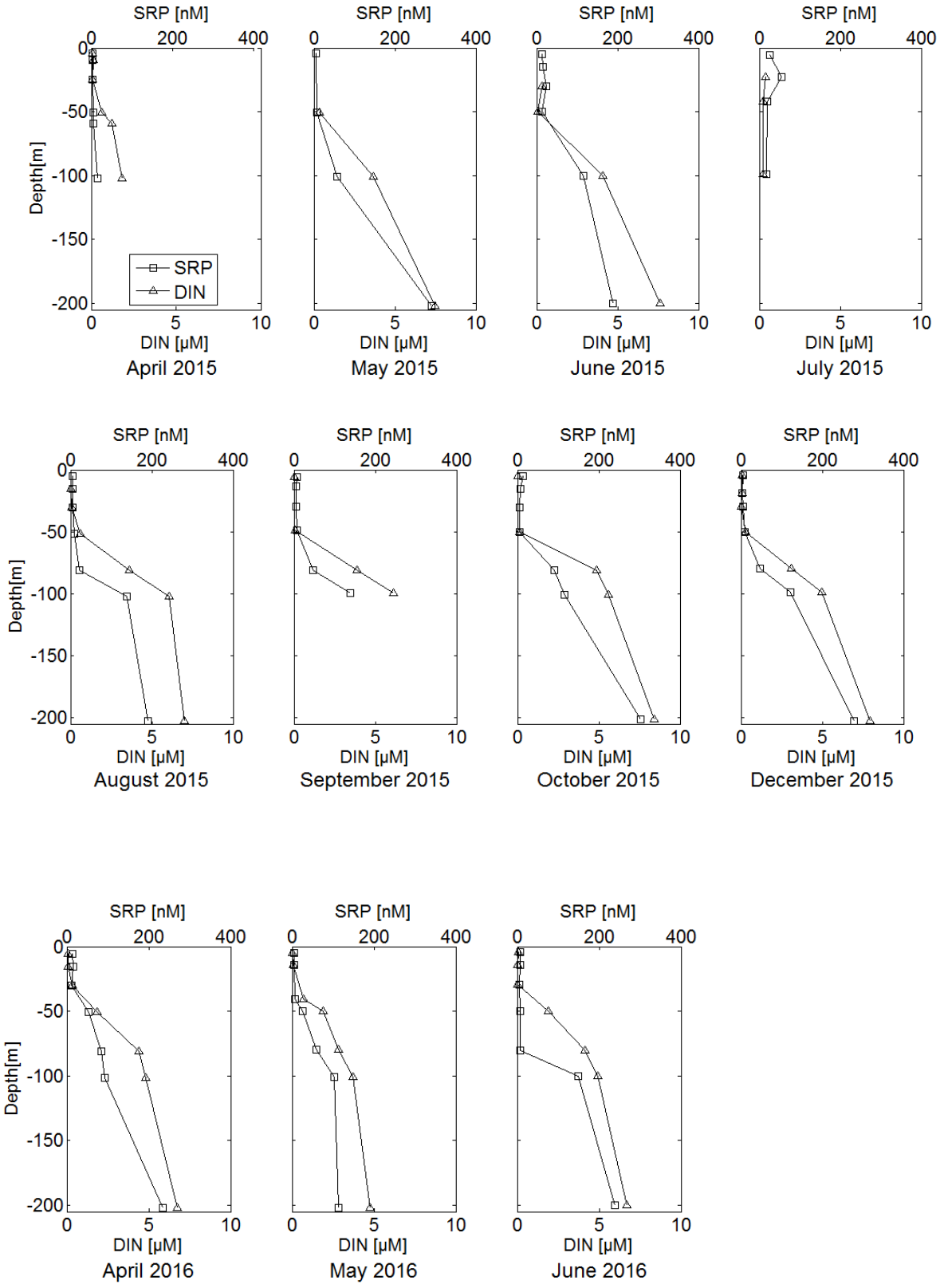
SRP [nM]
0
200
400
Depth[m]
-50
-100
-150
-200
SRP
DIN
DIN [µM]
0
5
10
April 2015
May 2015
June 2015
July 2015
August 2015
September 2015
October 2015
December 2015
April 2016
May 2016
June 2016

**Figure S5**

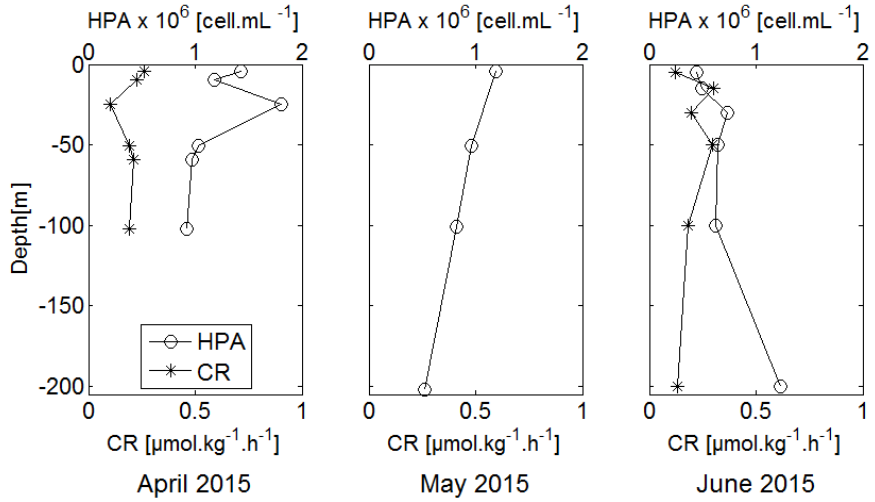
HPA x 10^6 [cell.mL^-1]
Depth[m]
HPA
CR
CR [µmol.kg^-1.h^-1]
April 2015
May 2015
June 2015

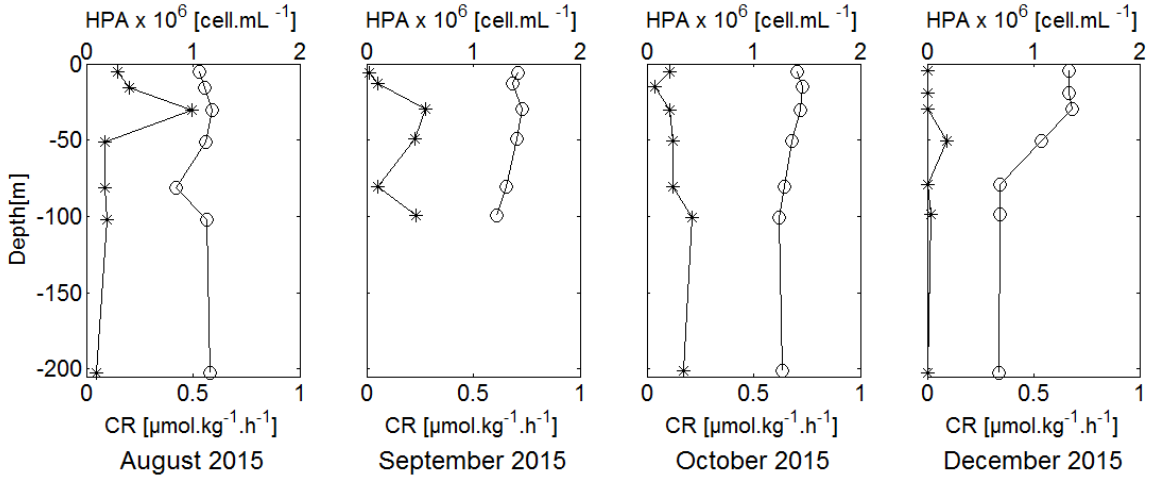
HPA x 10^6 [cell.mL^-1]
Depth[m]
CR [µmol.kg^-1.h^-1]
August 2015
September 2015
October 2015
December 2015

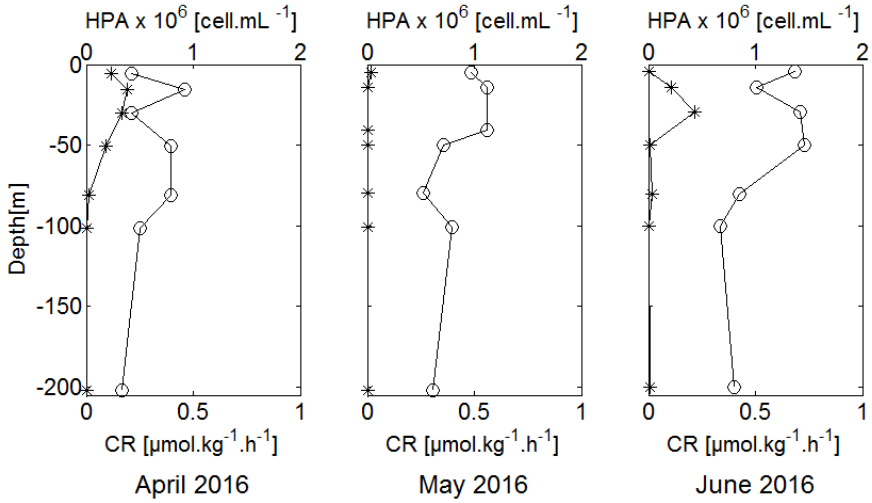
HPA x 10^6 [cell.mL^-1]
Depth[m]
CR [µmol.kg^-1.h^-1]
April 2016
May 2016
June 2016

**Figure S6**

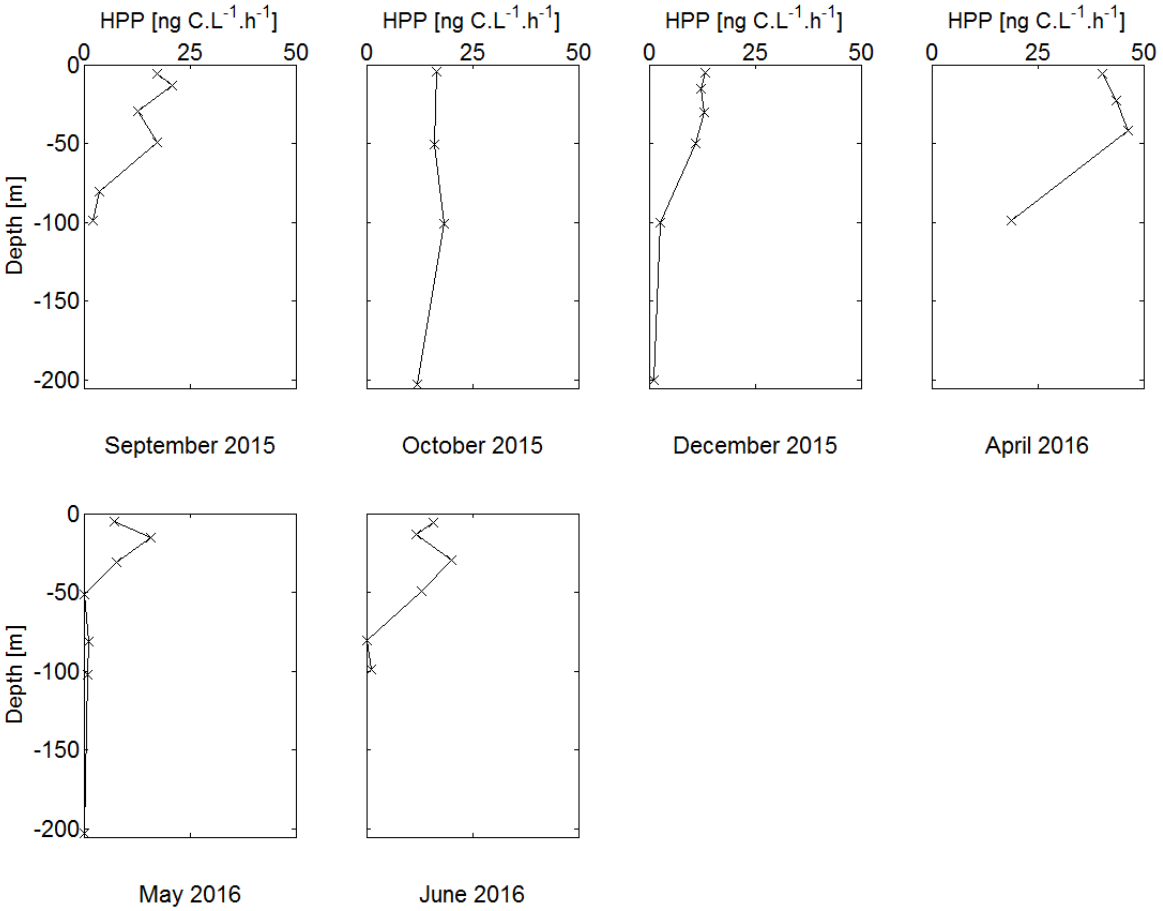
HPP [ng C.L-1.h-1]
0
25
50
0
-50
-100
-150
-200
Depth [m]
September 2015
October 2015
December 2015
April 2016
May 2016
June 2016